



Project title:

**Energy-Specific Solar Radiation Data
from Meteosat Second Generation (MSG):
The Heliosat-3 Project**

Project Acronym:

HELIOSAT-3

Contract No.:

NNK5-CT-2000-00322

Project No.:

NNE5-2000-00413

Title:

Final report

Deliverable:

D17

Authors:

**Jethro Betcke, Rolf Kuhlemann, Annette Hammer,
Anja Drews, Elke Lorenz, Marco Girodo,
Detlev Heinemann,
Lucien Wald, Sylvain Cros,
Marion Schroedter-Homscheidt, Thomas Holzer-Popp,
Gerhard Gesell, Thilo Erbertseder,
Miriam Kosmale, Beate Hildenbrand,
Knut-Frode Dagestad, Jan Olseth,
Pierre Ineichen,
Christian Reise,
Dominique Dumortier, Frans van Roy,
Antonio Ortegon Gallego
Hans Georg Beyer,
Franz Trieb, Christoph Schillings,
Carsten Hoyer, Stefan Kronshage
Hermann Mannstein, Luca Bugliaro, Waldemar Krebs**

Date:

January 2006



Energy and Semiconductor Research Laboratory
Carl von Ossietzky University of Oldenburg
D-26111 Oldenburg, Germany
Tel: +49 (0)441-798 3402
Fax: +49 (0)441-798 3326
Web: <http://www.energiemeteorologie.de>

Final report of the Heliosat-3 project

Jethro Betcke, Rolf Kuhlemann, Annette Hammer,
Anja Drews, Elke Lorenz, Marco Girodo, Detlev Heinemann,¹
Lucien Wald, Sylvain Cros,²
Marion Schroedter-Homscheidt, Thomas Holzer-Popp, Gerhard Gesell,
Thilo Erbertseder, Miriam Kosmale, Beate Hildenbrand,³
Knut-Frode Dagestad, Jan Olseth,⁴
Pierre Ineichen⁵, Christian Reise,⁶
Dominique Dumortier, Frans van Roy,⁷
Antonio Ortegón Gallego,⁸ Hans Georg Beyer,⁹
Franz Trieb, Christoph Schillings, Carsten Hoyer, Stefan Kronshage,¹⁰
Hermann Mannstein, Luca Bugliaro, Waldemar Krebs¹¹

20th January 2006

¹Carl von Ossietzky University of Oldenburg, Energy and Semiconductor Research Laboratory

²Ecole des Mines de Paris / Armines, Groupe Teledetection et Modelisation

³Deutsches Zentrum für Luft- und Raumfahrt, Deutsches Fernerkundungsdatenzentrum

⁴University of Bergen, Geophysical institute

⁵University of Geneva, Group of Applied Physics

⁶Fraunhofer Institute for Solar Energy Systems

⁷Ecole Nationale des Travaux Publics de l'Etat Centre National de la Recherche Scientifique Département Génie Civil et Bâtiment

⁸Canary Islands Technological Institute, Energy, Water and Bioengineering Division, Renewable Energies Department

⁹Hochschule Magdeburg-Stendal (FH), Fachbereich Elektrotechnik

¹⁰Deutsches Zentrum für Luft- und Raumfahrt, Institut für Technische Thermodynamik

¹¹Deutsches Zentrum für Luft- und Raumfahrt, Institut für Physik der Atmosphäre

Preface and Reading Guide

This is the public version of the final report of the Heliosat-3 project. A version containing financial and organisational details has been provided to the European Commission.

The structure follows the Guidelines for Reporting of the European Commission Fifth Framework program [European Commission, 2000]. Chapter one gives the background of the project and Chapter two the objectives. The scientific results are described in chapter three, the conclusions in chapter four. Dissemination and exploitation of results are described in the last chapter.

The Heliosat-3 project has been supported by the European commission within the fifth framework research program under contract number NNK5-CT-2000-00322.

Executive summary

Accurate solar irradiance data with a high temporal and spatial resolution is an essential input for the potential assessment, design, planning and performance monitoring of solar energy systems. Availability of these data is therefore of strategic importance for the market penetration of solar energy systems. The existing Heliosat-1 and Heliosat-2 methods provide irradiance data on the basis of earth observations from the geostationary Meteosat first generation. The methods are largely empirical and only use data from the visible light channel of Meteosat. For the application to the calculation of solar irradiance the new Meteosat generation has two major advantages over the previous generation: an increased spatial and temporal resolution and the availability of twelve spectral channels that can be used to obtain information about the composition of the atmosphere and the characteristics of clouds. Additional atmospheric data can be obtained from polar orbiting satellites such as ENVISAT and ERS.

To fully exploit the improved capabilities of MSG a new irradiance scheme is required. The main goal of the Heliosat-3 project is to develop such a new irradiance scheme and achieve an accuracy for global horizontal irradiance of less than 5, 10 and 20% for monthly, daily and hourly data, respectively. The new scheme aims to deliver direct normal irradiance, spectrally resolved irradiance, angular distribution of diffuse irradiance and the spatial structure of irradiance, as well. Secondary goals of the project are the implementation of the scheme in processing chains to end-user products, availability of retrieved cloud and atmospheric data for other purposes, providing an user interface, and dissemination of the results.

The Heliosat-3 consortium successfully developed an operational irradiance scheme on the basis of Meteosat Second Generation data. The scheme consists of the new SOLIS clear sky scheme, an MSG-adapted and improved cloud index scheme and a new all weather scheme. The scheme provides spectrally resolved global horizontal irradiance, and spectrally resolved diffuse horizontal irradiance. The data has a spatial resolution of of 1 km x 1km (nadir) and a temporal resolution of 15 minutes.

The clear sky scheme is based on radiative transfer modelling and provides spectrally resolved global and direct clear sky irradiance. It requires information on the aerosol, water vapour and ozone content of the atmosphere as input. In the current operational scheme climatological data are used. However, (near) real time data can be easily incorporated.

Besides technical changes to the software, adaptation of cloud index method to

MSG required solving problems with the geolocation of MSG-hrv images and a new determination of empirical parameters such as the maximal cloud reflectivity and the half-width of the ground reflectivity distribution.

Further improvements of the cloud index method have been developed: a correction for cloud shades, a new way to determine cloud reflectivity based on radiative transfer physics and a new statistic way to determine ground reflectivity. These improvements were not ready when the operational scheme had to be defined, but will be stepwise integrated in the operational scheme after the project.

The all-weather module includes a diffuse irradiance model that uses the newly available clear sky direct irradiance as input. Furthermore it includes a spectral look-up table to correct the spectral distribution of the clear sky irradiance for the presence of clouds.

The operational method was validated with pyranometer data from European meteorological stations. The accuracy goals set in the proposal, an RMSE of 20%, 10%, and 5% for hourly, daily and monthly values of global horizontal irradiance have been achieved for most test-sites. The use of MSG-data rather than Meteosat-7 data resulted in a reduction of the RMSE of hourly data of on average 1.5% (percent point). For north-west European test sites the results of the Heliosat-1 and operational Heliosat-3 methods were comparable. For Mediterranean and Canary island test sites the new method gave an RMSE reduction of approximately 2 %.

For diffuse irradiance the new method on average reduced the RMSE with 1.5 % compared to Heliosat-1.

Illuminance derived from the spectral product of the operational Heliosat-3 method was validated on ground measured data and compared with the Perez luminous efficacy model. It was found that the latter gave more accurate results. It is expected that a more appropriate choice of spectral bands and the use of Near Real Time atmospheric data will improve the results of the operational Heliosat-3 method.

It was investigated if the ground measured angular distribution of diffuse irradiance could be correlated to the spatial distribution of the cloud index. It was found that traditional hemi-sphere models are still more effective.

The spatial structure of the irradiance was investigated by comparing the cross-statistics of ground measured irradiance at two locations with the cross-statistics of Heliosat-3 determined irradiance for the same two locations. It was found that both match very well. However, it is necessary to develop a correction procedure to improve temporal dynamics of the Heliosat-3 procedure.

Application of the new product to the performance evaluation of grid-connected PV-systems and the assessment of the potential for solar thermal power plants illustrated the benefits of the new product.

The operational Heliosat-3 method has been implemented successfully the solar energy processing chain at Oldenburg University and the climatological processing chain in at Ecole de Mines. Moreover, the scheme is applied at the EUMETSAT Climate Satellite Application Facility at DWD.

The operational scheme differs from the scheme in the project proposal. The orig-

inal 'target' scheme would have had near real time atmospheric data as input to the clear sky module and a completely new cloudy sky scheme on the basis of advanced cloud information provided by the APOLLO scheme. Technical problems with the MSG satellite caused a large delay in the data availability. Consequently, the modules for the 'target' scheme were not ready at the start of the operationalisation and validation. However, they could be developed and validated componentwise in parallel to the validation of the operational scheme.

The Kleespies and McMillan method for water vapour retrieval has been adapted to the MSG-SEVIRI instrument and further improved. The method was validated on radiosonde measurements. With an RMSE of 6mm the results are in the required accuracy range.

To obtain aerosol information for the observation area of MSG, the SYNEAR method has been adapted to the polar orbiting satellite ERS-2 and ENVISAT. The method has been extended further to include new and more detailed aerosol types. An climatology has been prepared on the basis of historic data. This climatology has been used as input for the operational Heliosat-3 method. Validation of the ENVISAT-SYNAER version showed a large reduction of bias towards nearly zero and of standard deviation to 0.1. a.

A scheme for the retrieval of the total ozone column has been developed on the basis of the 3D global chemical-transportmodel DLR-ROSE 3.0 and data from ENVISAT-SCIAMACHY and ERS-2-GOME. The standard deviation for the GOME - WOUDC comparison is between 2.6 and 6.3 % with a mean deviation from -4.1 to 0.4 % depending on the reference station. For the SCIAMACHY - WOUDC comparison the mean deviation ranges from -8 to -0.8 % depending on the station. The standard deviation varies from 3.5 to 10.2 %.

The APOLLO scheme, which was originally developed to use data of polar orbiting satellites, has been adapted to the MSG-SEVIRI instrument. It provides a cloud mask, cloud optical depth, cloud fraction, cloud top temperature and cloud type. Cloud fraction was compared with NOAA-AVHRR data. Cloud Mask was compared with the MeCiDa algorithm. Both comparisons showed a good agreement.

The SOLIS CloudS scheme uses the cloud optical depth provided by APOLLO as input and based on a parametrisation of radiative transfer modelling. It is currently only valid for total overcast situations. A case study validation looks promising, but the cloud index method is still more accurate. Further development of APOLLO and SOLIS CloudS is necessary and will take place in the vIEM and ENVISOLAR projects.

The results of the project have been disseminated via publications, the website and a workshop. The products are exploited in end-use products and further developed in a number of projects.

Contents

1	Background	8
2	Scientific/technological and socio-economic objectives	9
2.1	Objectives	9
2.2	Contribution to EU policies	10
3	Applied methodology, scientific achievements and main deliverables	12
3.1	Introduction	12
3.1.1	Heliosat-3 irradiance scheme	12
3.1.2	Structure of this chapter	13
3.2	Retrieval of Cloud Mask and Cloud Optical Properties (WP 2020)	16
3.2.1	APOLLO	16
3.2.2	Adaptation of APOLLO to MSG-SEVIRI	17
3.2.3	Validation of the APOLLO output	18
3.3	Retrieval of Water Vapour (WP 2030)	18
3.3.1	Development	18
3.3.2	Validation	19
3.4	Retrieval and parametrisation of Aerosol Amount and Type (WP 2040)	21
3.4.1	Development	21
3.4.2	Validation	23
3.5	Retrieval of Ozone (WP2050)	23
3.5.1	Development	23
3.5.2	Validation	24
3.6	The SOLIS clear sky module (WP 3010)	24
3.6.1	Approach	24
3.6.2	Software implementation	26
3.6.3	Validation	26
3.7	Adaptation and improvement of the existing Cloud Index method (WP 3020)	28
3.7.1	Adaptation of the cloud index method to MSG	28
3.7.2	Development of an alternative cloud index algorithm	29
3.7.3	Correction for cloud shades	33
3.7.4	Variability correction for cloud index method	34

3.8	New COD based cloudy sky scheme: CloudS (WP 3020)	35
3.8.1	Development	35
3.8.2	Validation	36
3.9	The all weather module (WP 3020 / 3030)	39
3.9.1	Technical adaptations	39
3.9.2	Direct and diffuse irradiance (WP 3030)	39
3.9.3	Spectrally resolved all weather irradiance (WP3040)	39
3.10	Angular distribution (WP3030)	39
3.11	Spatial irradiance structure (WP 3050)	40
3.11.1	Measures for the local spatial variability of the irradiance field	40
3.11.2	Spatial statistics of irradiance data	42
3.12	Solar Energy processing Chain (WP 4010)	42
3.13	Climatological Processing Chain (WP 4020)	43
3.14	Validation of the operational Heliosat-3 irradiance calculation scheme (WP 5020)	45
3.14.1	Operational Heliosat-3 irradiance scheme	45
3.14.2	Global horizontal irradiance	48
3.14.3	Diffuse and direct Irradiance	51
3.14.4	Illuminance	52
3.14.5	Irradiance and illuminance on a tilted plane	52
3.14.6	Conclusions	53
3.15	Example Application: Grid Connected Photovoltaic Systems	54
3.15.1	The PVSAT procedure	54
3.15.2	Algorithms and data needs	56
3.15.3	Current accuracy	56
3.15.4	Improvements in accuracy	57
3.16	Example Application: Solar Thermal Power Plants	57
3.16.1	Solar Thermal Power Plants	58
3.16.2	STEPS	58
3.16.3	STEPS applied to the Canary Islands	58
3.17	Example Application: Daylighting (WP 6030)	62
4	Conclusions	63
5	Dissemination and Exploitation of the results	67
5.1	Dissemination	67
5.1.1	Website	67
5.1.2	Workshop	67
5.1.3	Information package	67
5.2	Exploitation of results	68
5.2.1	EUMETSAT CM-SAF	68
5.2.2	Meteocontrol Safersun	68
5.2.3	Snow detection	68

5.2.4	PVSAT-2	68
5.2.5	vIEM	69
5.2.6	LBA	69
5.2.7	ENVISOLAR	69
5.2.8	Cloud and water vapour products at DLR	70
5.2.9	HelioClim/SoDa	70
5.3	Cumulative list of Publications	70
5.3.1	Peer reviewed articles	70
5.3.2	Theses	71
5.3.3	Reports on Deliverables	71
5.3.4	Conference papers	73
5.3.5	Other publications	74
5.3.6	Planned publications	75
A	Participant Information	83
B	Glossary	88
C	Workshop Program	90

Chapter 1

Background

To achieve the goals of the EU energy policy and to accelerate the market penetration of solar energy technologies, improvements in both technological domains (e. g. to increase efficiency, to achieve mass production) and in the operation of solar energy systems are necessary. Detailed knowledge of the fluctuating energy source solar radiation is an issue of strategic importance for optimised system performance. Main limitations regarding the availability of high-quality solar radiation data have been identified by customers from solar energy industries:

- Uncertainty of local solar energy potential estimates is too high
- Spatial and temporal resolution of available radiation data is too low
- Solar energy specific information (direct normal and spectral irradiance,
- Angular distribution of diffuse irradiance, spatial structure) is commonly not available at all.

This lack of precise information frequently results in an incorrect system sizing, non-optimum site selection unreliable system performance, or unnecessary use of conventional energy sources. Consequently, the economic success of solar energy technologies are strongly influenced by these limitations. HELIOSAT-3 will supply high-quality solar radiation data gained from the exploitation of existing Earth observation technologies. Because of the increasing capabilities of these technologies, the expected quality represents a substantial improvement with respect to the available methods and will better match the needs of customers of the resulting products.

Chapter 2

Scientific/technological and socio-economic objectives

2.1 Objectives

The objectives of HELIOSAT-3 are:

- Provide a new surface solar irradiance calculation scheme according to customers requirements mentioned above. The forthcoming MSG satellite will be used to derive the actual atmospheric state. This information will be used in physically based parameterisation schemes for the solar radiation parameters, which are derived from extensive radiative transfer calculations. The enhanced capabilities of MSG with 12 spectral channels from the visible to the infrared, and higher resolutions in space (1 km) and time (15 min) allow this new approach.
- Reduce overall errors for global irradiance on a horizontal surface to less than 5,10, and 20 % RMSE on a monthly, daily, and hourly basis, respectively.
- Provide a set of up to now from satellite not available solar energy specific parameters: Direct normal and spectral irradiance, angular distribution of diffuse irradiance, spatial structure of irradiance.
- Implementation of an operational processing chain from MSG data to end-use products.
- Availability of retrieved data on clouds, water vapour, aerosols and ozone concentrations for other applications in global change and land use research, health monitoring, and weather forecasting.
- Provide an user interface based on WWW and GIS technology for easy access to HELIOSAT-3 results by the key customers, expert users and the public.
- Integration of results into existing efforts from EU and other projects and organisation of a users workshop.
- Optimisation of daylight usage in buildings

HELIOSAT-3 will significantly improve the planning and operating of solar energy technologies. This will be shown by example applications in co-operation with customers:

- Performance monitoring of grid-connected photovoltaic systems
- Planning and operation of concentrating solar thermal power plants
- Optimisation of daylight usage in buildings

2.2 Contribution to EU policies

The work performed within the project HELIOSAT-3 and its outcomes and achievements are relevant to the key action priorities in Theme 4: Energy, Environment and Sustainable Development, Key Action 5: Cleaner Energy Systems, Including Renewable Energies, Action Line 5.3: Integration of New and Renewable Energy Sources into Energy Systems. The HELIOSAT-3 project also contributes to ESD Part A: RTD Activities of a Generic Nature: Development of generic Earth observation technologies. The principle objective of HELIOSAT-3 is to support the solar energy community in its efforts for increasing the efficiency and cost effectiveness of solar energy systems and improving the acceptability of renewables. A successful integration of solar energy into the existing energy structure highly depends on a detailed knowledge of the solar resource. HELIOSAT-3 will significantly improve the current level of skill for solar irradiance estimation.

The follow-on generation of European operational geostationary satellites (Meteosat Second Generation, MSG) now provides a much better temporal, spectral and radiometric resolution and therefore presents the capabilities necessary for the retrieval of new and innovative solar radiation parameters. It allows the implementation of advanced physical retrieval algorithms for actual atmospheric and radiation parameters instead of using semi-empirical approaches for cloud and radiation parameters and climatologies for the other atmospheric parameters water vapour, aerosols and ozone. Furthermore, the synergetic use of atmospheric retrieval methods that have recently been developed separately for other Earth observation sensors is now possible.

Accurate solar radiation data derived from the new satellite generation will significantly improve most advanced solar energy applications like grid integration of photovoltaics, control of solar thermal power plants, future irradiance forecasting schemes, etc. It is expected that these new products will establish the primary solar radiation data source in the future. The expensive use of ground based pyranometer networks will be restricted to special investigations and high quality reference measurements at selected sites. HELIOSAT-3's advantage lies in following a highly multidisciplinary approach through the collaboration of users and scientists from the energy sector to-

gether with scientists working on the field of atmospheric physics. It therefore leads to new products and new expertise and shows how Earth observation will fill information gaps. The expected results of HELIOSAT-3 demonstrate the potential to establish geostationary satellites as a primary data source for detailed surface solar radiation data used in solar energy applications. They extend the European capacity in Earth observation through the development of new information sources for the energy sector. The use of renewable energies will be supported and therefore the use of fossil fuels will be reduced. This is a major contribution to the protection of our environment and improves quality of life.

Chapter 3

Applied methodology, scientific achievements and main deliverables

3.1 Introduction

3.1.1 Heliosat-3 irradiance scheme

The visible channel of the radiometer on board the weather satellite Meteosat-7 provides earth images every half hour. Sub-satellite the spatial resolution is $2.5 \text{ km} \times 2.5 \text{ km}$, for North Western Europe this is approximately $2.5 \text{ km} \times 4 \text{ km}$. The operationally working methods Heliosat-1 [Fontoynt, 1998, Hammer et al., 2003] and Heliosat-2 [Rigollier et al., 2004, Rigollier et al., 2001] use statistical methods and semi-empirical formulas to calculate solar irradiance. They calculate the clear sky irradiance on the basis of a turbidity climatology. The actual irradiance is determined by multiplying the clear sky irradiance with the so-called cloud index which is derived by an empirical method from the Meteosat images. The Heliosat-1 scheme is illustrated in Figure 3.1.1.

The SEVIRI instrument on board the Meteosat Second Generation (MSG) offers not only a higher spatial and temporal resolution of the broadband visible (HRV) channel, $1 \text{ km} \times 1 \text{ km}$ and 15 Min respectively, but also an extensive range of narrow band visible and infrared channels. These channels allow for the retrieval of water vapour and ozone content of the atmosphere, and of detailed cloud characteristics such as cloud optical depth, cloud top temperature and cloud type. Information on aerosols can be derived from instrument on board of the polar orbiting satellites such as Envisat and ERS-2.

The newly available data on atmospheric and cloud parameters allow for the development of a new irradiance calculation scheme based on radiative transfer modelling (RTM). RTM based schemes hold the potential for greater accuracy of the global and direct irradiance, and additionally open the possibility to produce spectrally resolved data.

Such a scheme was the original target of the Heliosat-3 project. It is illustrated

in Figure 3.1.1. The general structure of the scheme is the same as in the Heliosat-1 scheme: it consists of a clear sky module, a cloud module and an all weather module that combines the results of the first two modules to obtain the actual irradiance. One of the advantages of this modular structure is that the clear sky and the cloud module can be independently developed and exchanged.

However, due to delay in launch and data-transmission of Meteosat-8 (a.k.a. MSG-1), the RTM based cloud module could not be completed before the start of the validation of the overall scheme. On these grounds the consortium decided to validate the combination of the new SOLIS clear sky module and an adapted version of the existing Heliosat-1 cloud index method. For similar reasons was it not possible to have near real time atmospheric data for the period over which the scheme was validated. Climatological data were used instead. This 'operational' Heliosat-3 scheme is illustrated in Figure 3.1.1.

The development of the target scheme continued in parallel to the validation of the operational scheme. The atmospheric data modules and the APOLLO module could be completed and validated separately. The CloudS module could be completed for the limited case of total overcast cloud situations. Further development and validation of the target Heliosat-3 scheme is currently ongoing as part of the vIEM and ENVI-SOLAR projects.

3.1.2 Structure of this chapter

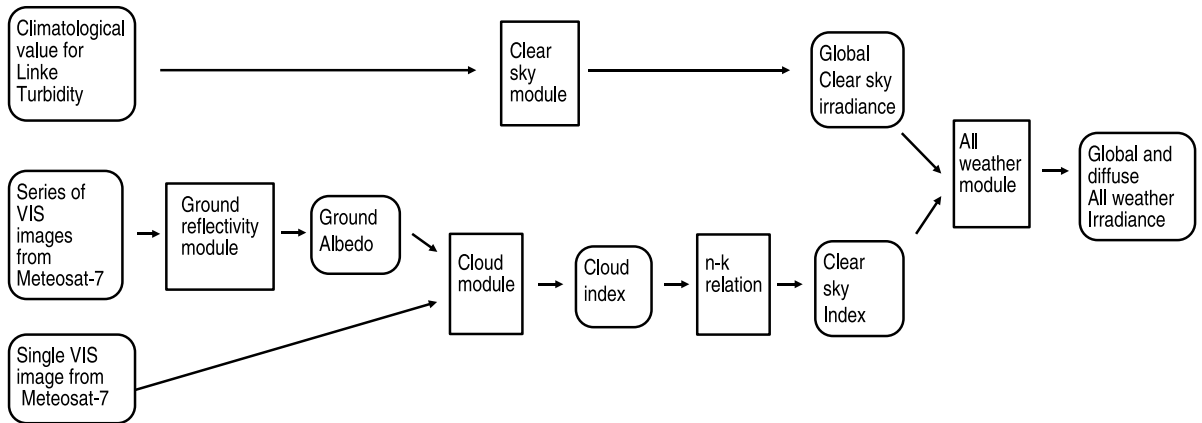
The SOLIS clear sky module, which is part of the target and the operational Heliosat-3 scheme, is described in Section 3.6. The adapted and improved version of the existing Heliosat-1 cloud index method (Sunsat), which is part of the operational scheme, in Section . Extensions of the operational scheme to determine the angular distribution and the spatial structure of the irradiance can be found in 3.10 and 3.11.

The validation of the operational scheme is described in 3.14. Example applications of the operational scheme are described in Sections 3.17 to 3.17.

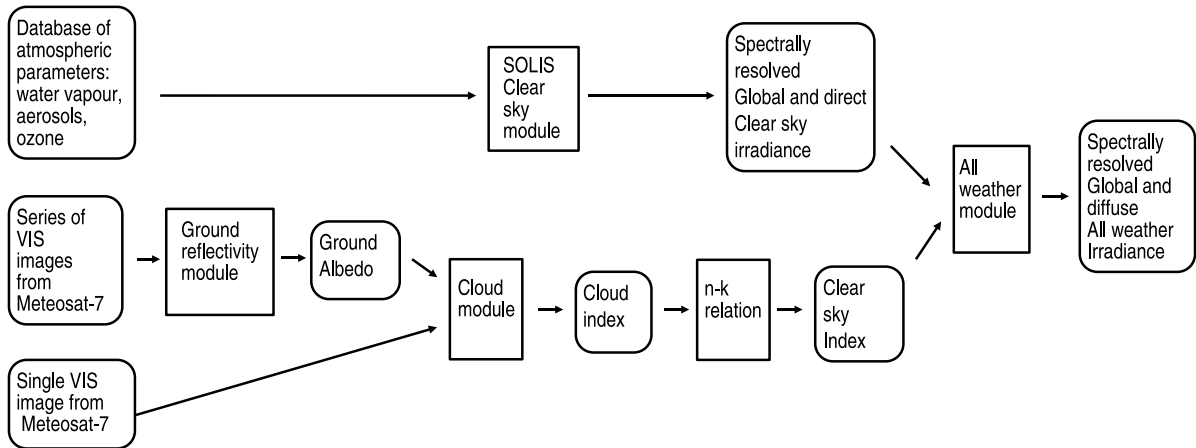
The development of methods for the retrieval of atmospheric clear-sky parameters and cloud physical properties, which are part of the target scheme, are described, in the Sections 3.2 to 3.5.

The order of the sections corresponds with the order of the work packages in the project.

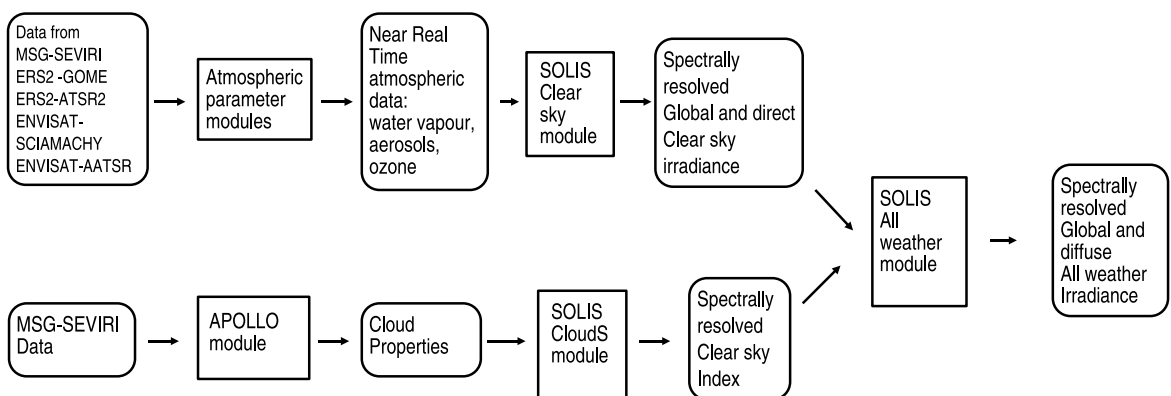
Most deliverables are also described in separate technical reports. Table 3.1 gives an overview of all deliverables of the Heliosat-3 project.



(a) Heliosat-1 scheme



(b) Heliosat-3 operational scheme



(c) Heliosat-3 target scheme

Figure 3.1: An overview of the new Heliosat-3 scheme. The rounded boxes depict data, the rectangular boxes software.

Table 3.1: Deliverables of the Heliosat-3 project.

Nr.	Title	Reported in
D 1	management plan	
D 2	compilation of data requirements	Report [EHF and Ecole de Mines/Armines]
D 3	Internet presentation	www.Heliosat3.de, Report [EHF, 2001]
D 4	Dissemination plan/TIP	electronically via e-TIP
D 5	Scientific publications	Ch. 5.3
D 6.1	Cloud processing scheme, working version	Report [Heliosat-3 consortium, 2002]
D 6.2	Water vapour retrieval scheme, working version	Report [Heliosat-3 consortium, 2002]
D 6.3	Aerosol parametrisation scheme, working version	Report [Heliosat-3 consortium, 2002]
D 6.4	Ozone processing scheme, working version	Report [Heliosat-3 consortium, 2002]
D 7	Mid-term progress report	Report [Heliosat-3 consortium, 2002]
D 8.1	Heliosat3 software clear sky, working version	Report [Heliosat-3 consortium, 2002]
D 8.2	Heliosat3 software all sky, working version	Report [EHF et al., 2003]
D 9.1	Cloud processing scheme, final version	Section 3.2 Report [Schroedter- Homscheidt, 2004]
D 9.2	Water vapour retrieval scheme, final version	Section 3.3 Report [Schroedter- Homscheidt, 2004]
D 9.3	Aerosol parametrisation scheme, final version	Section 3.4 Report [Schroedter- Homscheidt, 2004]
D 9.4	Ozone processing scheme, final version	Section 3.5 Report [Schroedter- Homscheidt, 2004]
D 10	Heliosat3 information package	Section 5.1.3
D 11.1A	Algorithms for direct and diffuse irradiance	Integrated in D8.2
D 11.1 B	Angular distribution of diffuse irradiance	Report [Ineichen, 2005b]
D 11.2	Algorithms for calculation of spectrally filtered solar irradiance data	Section 3.9.3
D 11.3	Algorithms for inference of spatial irradiance structure	Section 3.11 Report [Beyer et al., 2005]
D 12.1	Heliosat 3 software clear sky, final version	Section 3.6
D 12.2	Heliosat 3 software all sky, final version	Section 3.7.1 3.7.2, 3.7.3 and 3.8

Nr.	Title	Reported in
D 13.1	Routine processing chain for solar energy specific data	Section 3.12 Report [Kuhlemann et al., 2005] Report [Kuhlemann and Hammer, 2005]
D 13.2	Routine processing chain for climatology oriented data	Section 3.13 Report [Wald, 2005]
D14	Workshop	Section 5.1.2
D 15.1	Example Application No. 1: Performance evaluation of Grid Connected PV systems	Section 3.15
D 15.2	Example Application No. 2: Solar Thermal Power Plants	Section 3.16 Report [Schillings, 2005]
D 15.3	Example Application No. 3: Daylightning	Section 3.17 Report [Dumortier and van Roy, 2005]
D 16	Validation report	Section 3.14 Report [Dagestad et al., 2005]
D 17	Final report	this document

3.2 Retrieval of Cloud Mask and Cloud Optical Properties (WP 2020)

3.2.1 APOLLO

The AVHRR Processing scheme Over cLOUDs Land and Ocean (APOLLO, [Saunders and Kriebel, 1988], [Kriebel et al., 1989], [Gesell, 1989], [Kriebel et al., 2003]) was originally developed to make use of the AVHRR instrument on board of polar orbiting satellites of the NOAA series. It was the first AVHRR data processing scheme to make use of all five spectral channels during daytime. It discretises all pixels into four different groups called cloud-free, fully cloudy, partially cloudy (i.e. neither cloud-free nor fully cloudy) and snow/ice-contaminated, before deriving physical properties.

Within APOLLO, clouds are categorised into three layers according to their top temperature. The layer boundaries are set to 700 hPa and 400 hPa. The associated temperatures are derived from standard atmospheres. Further, each fully cloudy pixel is checked to see whether it is thick or thin cloud, depending on its 11 μm and 12 μm brightness temperatures and, during daytime, its channel 0.6 μm and 0.8 μm reflectances. Thin clouds (with no thick clouds underneath) are taken as ice clouds, i.e. cirrus, whereas thick clouds are treated as water clouds.

Cloud cover is derived for each cloud type separately. To derive the fractional cloud cover of the partially cloudy pixels at daytime, the relationship of the measured 0.6 μm and 0.8 μm reflectances to the mean of the fully cloudy and cloud-free reflectances in a local neighbourhood (e.g. 50 by 50 pixels) is used. More details of these methods

are given in [Saunders and Kriebel, 1988].

At daytime, for each fully cloudy pixel, clouds optical depth, liquid/ice water path and IR-emissivity are derived by means of parameterisation schemes using the reflectance at $0.6 \mu\text{m}$. The parameterisation scheme is based on the directional hemispherical cloud top reflectance, which is obtained from the (measured) bi-directional top of atmosphere reflectance by applying an anisotropy correction, correction due to ozone absorption and subtracting the surface part of the reflectance transmitted through the cloud. Details of the method can be found in [Kriebel et al., 1989].

3.2.2 Adaptation of APOLLO to MSG-SEVIRI

The AVHRR instrument on polar orbiting satellites has a daily global coverage of the earth surface. This temporal resolution is too low for an operational irradiance calculation scheme such as Heliosat-3. A usable alternative is the SEVIRI instrument on board the geostationary satellite MSG. It offers a full earth disk scan every fifteen minutes similar to AVHRR. To use SEVIRI data as input for APOLLO technical changes in the software were necessary, as well as adaptations to the underlying physical models.

The technical changes dealt mainly with the other data formats and the difference in geometry between a geo-stationary and a polar-orbiting satellite.

The changes of the physical models of APOLLO to MSG-SEVIRI included the following:

- Defaults of thresholds for most of the APOLLO algorithms have to be set depending on the region covered by the data to be processed. The thresholds itself are either set explicitly or are dynamically derived from local histogram calculations in neighbourhood-boxes. Therefore, all explicitly set thresholds and default settings have been changed, i.e. their values have been adapted to the regions visible by SEVIRI (especially necessary for non-European areas). These presets must be physically reasonable, i.e. are climatologically or empirically determined for the complete SEVIRI view and usually depend on region and season.
- Step 2 and 3 in the APOLLO processing contain corrections for regional peculiarities, e.g. cold currents and thermal fronts in the ocean, deserts with frequent sand storms etc. These local peculiarities can cause misclassification and wrong values for the cloud parameters and the processing must correct for it. These corrections depend not just on the region with the certain peculiarity but also on the degree of experience with it. Therefore, each APOLLO processing scheme is specific for the region it is applied to and APOLLO/SEV and APOLLO/AVH differ here as much as the AVHRR-view (covering mainly Europe due to field-of-view of DLRs receiving system at Oberpfaffenhofen) and SEVIRI-view are different.

3.2.3 Validation of the APOLLO output

The quantities provided by Apollo are not available as, or difficult to compare with, ground measurements. Instead a comparison with established satellite methods has been made.

Apollo-MSG-SEVIRI cloud fraction was compared with Apollo-NOAA-AVHRR based data, i.e. same method, different satellite. It was found that over land the AVHRR cloud fractions tend to be higher, and over sea the MSG-SEVIRI data gave higher values. The differences between the two satellites were comparable with the differences found between ground determined data and the Apollo-NOAA-AVHRR based data.

Apollo-MSG cirrus mask was compared with the MeCiDa algorithm using MSG data, i.e. different method same satellite. The Apollo method showed a detection efficiency of 36% to 50% and a false alarm rate of 2%. This was to be expected since APOLLO does not consider cirrus clouds above low clouds, and the MeCiDa is more sensitive on thin cirrus clouds.

3.3 Retrieval of Water Vapour (WP 2030)

3.3.1 Development

Several retrieval methods to derive total water vapour content (TWC) over land from MSG SEVIRI data have been tested, using the Thermodynamic Initial Guess Retrieval (TIGR, [Chedin et al., 1985]) data set to represent possible atmospheric states of temperature and humidity distribution. The reference TWC could be calculated from these profiles.

The comparison indicated that a split window retrieval algorithm for the retrieval of water vapour column over land as published by Kleespies and McMillan [Kleespies and McMillan, 1990, Kleespies and McMillan, 1984] was best suited for MSG. The method uses the split window channels at 10.8 and 12 μm . In general, infrared measurements are affected by air temperature, surface temperature, surface emissivity, water vapour and absorption of other atmospheric gases. Split window channels are selected close to each other, so that equal emissivity and absorption of other gases than water vapour can be assumed. Surface temperature is the same for both channels as this parameter is not dependent of the observer's wavelength. This reduces the dependence of measurements in these channels to air temperature and water vapour absorption. Two situations with varying surface temperatures are selected and therefore, two brightness temperature measurements can be exploited. Having these two equations the air temperature dependence can be eliminated. MSG offers the possibility to use this approach as it measures in a 15 minutes temporal resolution and therefore, can deliver *two situations with varying surface temperatures* during the daily temperature cycle. Equations 3.1 and 3.2 describe the functional relationship between brightness temperatures and TWC.

$$\frac{\tau_{11}}{\tau_{12}} = \frac{T_{11}^A - T_{11}^B}{T_{12}^A - T_{12}^B} \quad (3.1)$$

$$TWC = fct\left(\frac{1}{\sec \theta} \ln \frac{\tau_{11}}{\tau_{12}}\right) \quad (3.2)$$

T is the brightness temperature in channel 11 or 12 μm , θ is the satellite zenith angle, A and B are two temporal different situations and τ stands for transmission. A minimum difference of 8 K between T_{12} in situation A and B is required to avoid noise effects. Kleespies and McMillan proposed a linear relationship between the transmission ratio term and TWC (Equation 3.2). Testing the whole TIGR data set it turned out that a third order polynomial describes the relationship better. Presumably, the reasons for this non-linear behaviour are (a) non-neglectable absorption of other atmospheric gases if TWC is very small and (b) saturation of absorption lines for large TWC values.

A significant dependence on satellite zenith angle was found. Especially for larger TWC values a simple cosine airmass correction as used in Equation.3.2 is not suitable anymore. An explicit calculation of airmass correction in the infrared needs detailed information about the temperature profile of the atmosphere. Unfortunately, this will not be available later in the operational processing scheme. Therefore, a parameterisation was developed. All coefficients of the third order polynomial can be parameterised with sufficient accuracy using a quadratic fit.

Figure 3.2 gives an example of the level 2 and level 3 water vapour column product. The level 2 product (top) contains the water vapour data that could be derived from MSG-SEVIRI. Please note, that the method derives TWC only over land which is most relevant for solar energy applications. Further data gaps are due to cloud cover. The level 3 product (bottom) is generated in a 3-step-approach: (1) average all level 2 data available in a 0.5×0.5 latitude/longitude grid box, (2) interpolate empty boxes locally, and (3) fill still empty boxes with a background climatology based on the NASA Water Vapour Project (NVAP) data set [Randel et al., 1996, Simpson et al., 2001].

3.3.2 Validation

Comparisons of MSG-SEVIRI based total water vapour columns with radiosonde measurements have been performed for an European subset of the MSG field of view and for the full field of view covering Europe and Africa. The radiosonde measurements have been collected by the Met Office (UK) and provided by the British Atmospheric Data Centre (BADC). They comprise vertical profiles of temperature and dew-point temperature at standard and significant pressure levels, which allow for the calculation of the total water vapour column.

The period investigated includes March 1st, 2004 to August 31st, 2004 for the European subset and May, July, and August 2004 for the full field of view data. For the whole study period a bias of -0.1 mm is found for level 2 data together with a

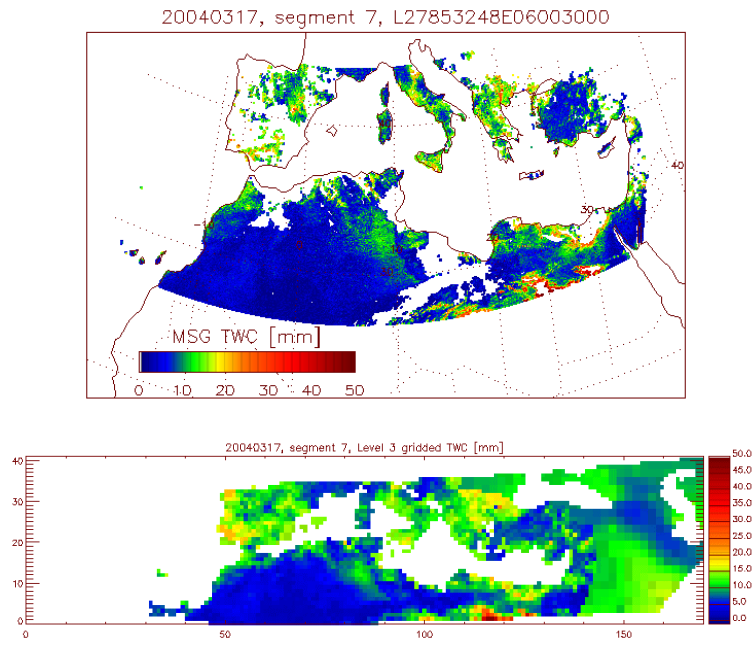


Figure 3.2: Examples of Level 2 (top) and Level 3 (bottom) water vapour products: MSG derived TWC in mm, March 17th, 2004.

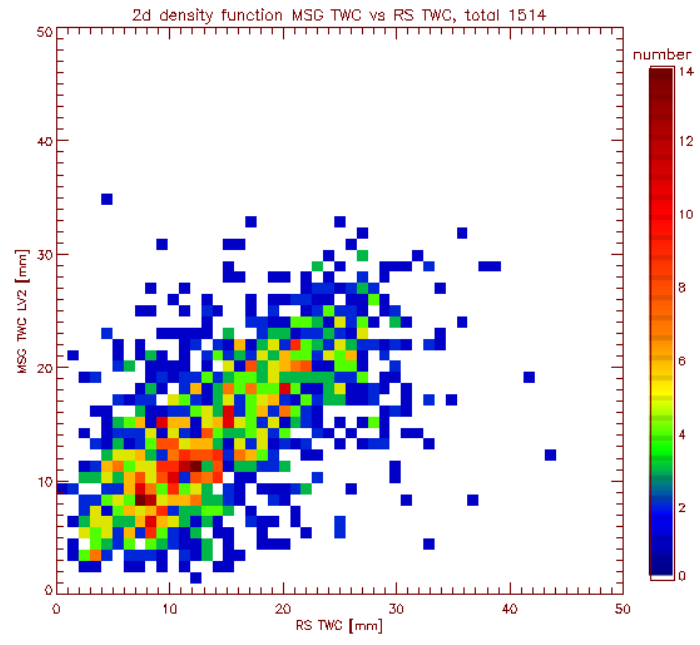


Figure 3.3: Two dimensional histogram of satellite level 2 data and radiosonde total water vapour column, period March-August2004, European and African radiosondes.

RMSE of 6.18 mm. For level 3 data the bias is -0.29 mm and the RMSE is 5.82 mm. The overall results are therefore within the range defined in the data requirements document for irradiance calculations.

Figure 3.3 shows the 2 dimensional histogram plot of satellite-based total water vapour column against radiosonde-based total water vapour column. A noteworthy scatter can be noticed which results in a low correlation coefficient of 0.63. Nevertheless, a maximum of coincidences can be clearly identified around the identity line. Having the required accuracy of less than 10 mm in mind, it can be stated that 96% of the differences are within a 10 mm range and even 83% are within an even stricter 5 mm range. Therefore, the accuracy requirement specified is fulfilled.

3.4 Retrieval and parametrisation of Aerosol Amount and Type (WP 2040)

3.4.1 Development

The goal of this work package is to create an aerosol climatology for the observation area of MSG that can be used as an input for the clear sky irradiance scheme. The aerosol information is obtained using the synergetic aerosol retrieval method (SYNAER), which exploits a spectrometer radiometer combination to retrieve aerosol optical thickness and type. SYNAER has originally been developed with GOME (Global Ozone Monitoring Instrument) and ATSR-2 (Along Track Scanning Radiometer), both on-board the polar orbiting European Radar Satellite ERS-2 [Holzer-Popp et al., 2002a, Holzer-Popp et al., 2002b]. The methodology selects the most plausible type of aerosols from remote sensing observations in each pixel without relying on any background data set.

The optical properties of the different aerosol particles are taken from the OPAC database [Hess et al., 1998]. However, within the HELIOSAT-3 project the SYNEAR method has been updated in the description of aerosol optical properties based on recent aerosol campaigns [Dubovik et al., 2002, Guyon et al., 2003, Moulin et al., 2001, Schnaiter et al., 2003]. These new aerosol models are currently included into the 'climatology data set'. Especially soot and mineral aerosols are now described more in detail and with extended focus on low and high absorbing aerosol types in both groups in the retrieval method.

A first climatology containing annual values for a five by five degree grid has been prepared. To enable the use of the SYNEAR data as input for libRadtran the detailed aerosol information is distilled to three parameters: the aerosol optical thickness at 550nm and the angstrom exponents α and β that describe the aerosol type.

A follow-up climatology containing with higher spatial and temporal resolution is being developed as part of the vIEM project.

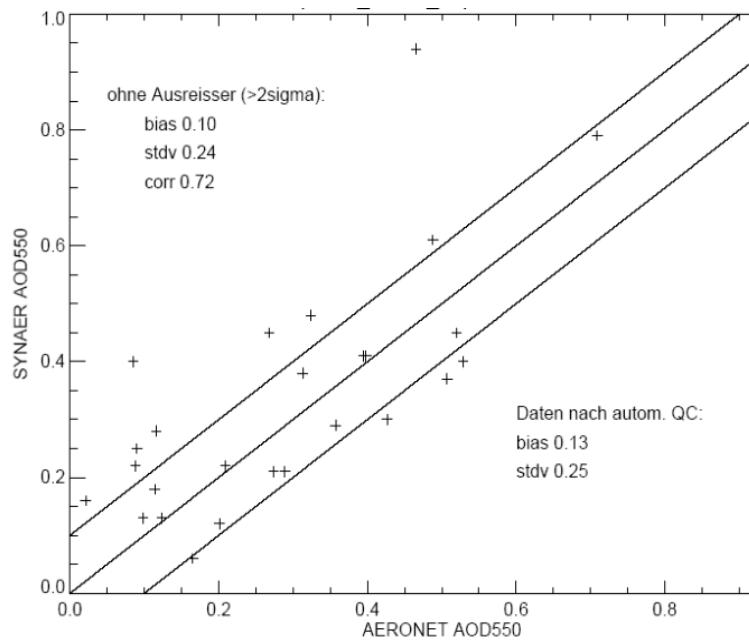


Figure 3.4: Scatterplot of SYNAER aerosol optical depth at 550 nm and AERONET ground measurements.

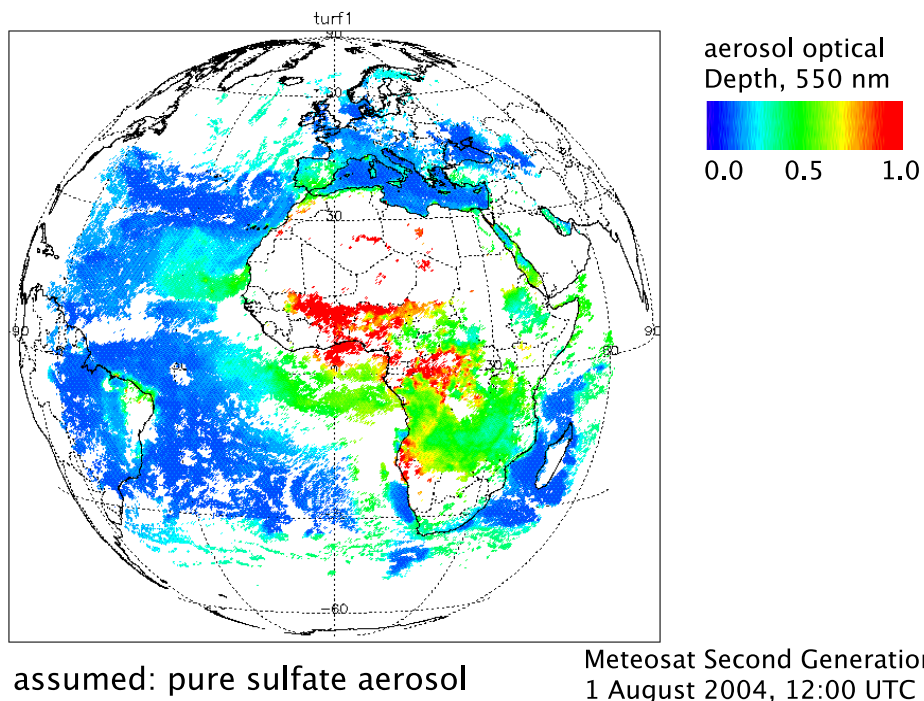


Figure 3.5: Example of SYNAER-SEVIRI results.

3.4.2 Validation

Validation of the SYNAER method in general have been carried out in first case studies distributed over the globe at 14 locations and one airborne lidar measurement show a good agreement with errors less than 0.1 in six wavelengths (340 - 870 nm) which indicates correct assessment of the amount and type (namely the spectral dependence of extinction) of aerosol. These results have already been published in [Holzer-Popp et al., 2002b] . Furthermore, a comparison of monthly mean results from SYNAER and other satellite aerosol retrievals as well as AERONET [Holben et al., 1998] stations over ocean [Myhre et al., 2005] showed a satisfactory agreement with the other data sets.

The comparison result for 29 cases of coincidence of the Heliosat-3 climatology data set and AERONET is given in Fig. 3.4. The general agreement is acceptable, but there is also a bias of 0.1 which shows that SYNAER tends to overestimate aerosol optical depth in comparison to AERONET measurements. The standard deviation between both measurements is 0.24 and the correlation coefficient is 0.72. To evaluate this further and to look more into details of possible failure reasons, further evaluation with a larger data set as expected from ENVISAT (daily products, 16 pixels per scan line instead of 3) is ongoing.

First results show an improvement based on ENVISAT data with a bias close to zero and standard deviation of 0.1. SYNAER has also been adapted successfully to MSG-SEVIRI assuming a constant aerosol type. Figure 3.5 gives an example for 1st August 2004, 12 UTC.

3.5 Retrieval of Ozone (WP2050)

3.5.1 Development

Ozone total column data is provided by SCIAMACHY aboard ENVISAT. SCIAMACHY is a spectrometer measuring atmospheric absorption in spectral bands from the ultra-violet to the near infrared (240 nm - 2380 nm). From these observations total column amounts and stratospheric profiles of a multitude of atmospheric constituents are retrieved on a global scale [DLR, 2000]. Currently, SCIAMACHY data of version 5.04 is available. Due to the scanning geometry of SCIAMACHY total column ozone observations are heterogeneously distributed in time and space. In order to gain synoptic distributions of total column ozone considering atmospheric variability the SCIAMACHY observations are sequentially assimilated into a 3D chemistry-transport model, describing all relevant chemical and physical processes [Erbertseder, et al. 2004, Erbertseder et al.,2003].

The 3D global chemical-transport model DLR-ROSE 3.0 is used. It is based on the ROSE model described in detail in [Rose and Brasseur,1989,Riese et al.,1999], but was significantly improved. The model covers all relevant gas-phase stratospheric chemical processes. Heterogeneous processes are also included in the model. It accounts

for about 100 reactions, including oxygen, hydrogen, carbon, nitrogen chlorine, and bromine species. The basic chemical time-step is 15 minutes. All species are transported every 90 minutes using a Lin and Rood scheme. The model is driven by wind and temperature fields of the European Center for Medium Range Weather Forecast (ECMWF). The spatial discretisation of the DLR-ROSE 3.0 uses a $2.8^\circ \times 2.5^\circ$ lon.-lat. spherical grid and 43 log-pressure levels between 0 and 56 km altitude (316. to 0.316 hPa) resulting in a vertical step size of 1.3 km. Globally gridded 3D ozone as well as total column ozone fields are available every 6 hours. As backup to SCIAMACHY observations for the Global Ozone Monitoring Experiment (GOME, currently available in version 4.0) can be applied. As from mid of 2006 observations from the upcoming GOME-2 instrument aboard METOP will be used.

3.5.2 Validation

Total ozone measurements archived at the World Ozone and UV Data Center (WOUDC) in Toronto, Canada [woudc,2005] are used as reference for the validation. The WOUDC dataset contains total ozone data mainly from Dobson and Brewer UV spectrophotometers and from M-124 UV filter radiometers. To prepare ground-based data sets for the sake of GOME and SCIAMACHY validation, we investigated the quality of 10 total ozone data records of stations distributed over all latitude regions. For GOME ground-based data of the year 2000, for SCIAMACHY of 2003 was applied.

The general agreement of SCIAMACHY is very good, the agreement of GOME excellent, reaching the accuracy of ground-based measurements. Over the middle and high latitudes of both hemispheres SCIAMACHY overestimates ground-based total ozone during winter-spring. During summer-autumn it underestimates ground-based ozone values. In the tropics there was no significant seasonal dependence of the differences observed but in general ozone was slightly underestimated by SCIAMACHY. Recapitulating the relative differences ((satellite-ground-based)/satellite) SCIAMACHY usually does not exceed 10% for individual values.

The standard deviation for the GOME - WOUDC comparison is between 2.6 and 6.3 % with a mean deviation from -4.1 to 0.4 % depending on the reference station. For the SCIAMACHY - WOUDC comparison the mean deviation ranges from -8 to -0.8 % depending on the station. The standard deviation varies from 3.5 to 10.2 %.

3.6 The SOLIS clear sky module (WP 3010)

3.6.1 Approach

In the Heliosat-1 method the global clear sky irradiance is determined with the empirical Dumortier model [Dumortier, 1995] that uses climatological values of the Linke turbidity factor as input.

The availability of data on the aerosol, water vapour and ozone content of the atmosphere makes it possible to calculate the clear sky irradiance using radiative transfer modelling. This not only opens the door to a higher accuracy, but also provides information not available with the Heliosat-1 model: spectrally resolved global and direct irradiance.

However, to use RTM for every point in a time-series or irradiance map would be too slow for operational use. Furthermore, the data describing the state of the atmosphere are mostly only available on spatial and temporal scales larger than the scales required for the irradiance data sets.

Therefore, the new SOLIS clear sky module [Mueller et al., 2003] uses a more practical approach:

1. The uvspec solver from the RTM library libRadtran [Mayer and Kylling, 2005] is used to calculate direct and diffuse in each of the Kato correlated-k wavelength bands [Kato et al., 1999], for the solar zenith angles 0° and 60° . Water vapour, aerosol and ozone information are used as input. Currently, these data are taken from a climatology. But, when available, they can be given by a near real time (NRT) scheme.
2. On these two points the modified Lambert Beer (MLB) functions are fitted:

$$I_{direct} = I_0 * \exp\left(\frac{\tau_{0d}(\lambda)}{\cos^{a(\lambda)}(\theta_z)}\right) * \cos(\theta_z) \quad (3.3)$$

$$I_{global} = I_0 * \exp\left(\frac{\tau_{0g}(\lambda)}{\cos^{b(\lambda)}(\theta_z)}\right) * \cos(\theta_z) \quad (3.4)$$

$$I_{diffuse} = I_0 * \exp\left(\frac{(\tau_{0diff}(\lambda))}{\cos(\theta_z)^{c(\lambda)}}\right) \quad (3.5)$$

where: I_0 is the extra-terrestrial irradiance, λ is the wavelength, θ_z is the solar zenith angle, τ_{0d} , τ_{0g} and τ_{0diff} are the (wavelength dependent) effective optical depths at $\theta_z = 0$ for direct, global and diffuse irradiance, respectively. and a , b and c are the (wavelength dependent) MLB parameters. τ_{0d} , τ_{0g} , τ_{0diff} , a , b and c are the free parameters for the fit.

3. With known effective optical depths and MLB parameters the clear sky irradiance can be calculated very quickly for any solar zenith angle. And thus for any place and time with an atmospheric condition similar as for which the original RTM calculation was carried out.

At low visibilities (high optical depth, high aerosol load) a correction on I_0 has to be applied for global and diffuse radiation. For that purpose a general formula has been developed.

3.6.2 Software implementation

The SOLIS module consists of the following parts:

- a library of c- programs that can read the appropriate atmospheric data from the files
- an installation of the program library libRadtran
- the awk programs convert.awk and convert-l.awk that fit the MLB functions to the RTM-calculated irradiance
- the central script kato.sh that prepares the libRadtran input using the database interfaces; calls libRadtran followed by a call to convert.

The actual calculation of the clear sky irradiance from the MLB parameter takes place in the all weather module *n2irr*.

3.6.3 Validation

The first step in the validation is to investigate the validity of the MLB fit [Mueller et al., 2003]. Figure 3.6 shows that the MLB functions reproduce the results of a RTM calculation very well.

The second step is to investigate the ability of SOLIS to reproduce the diurnal variation of the clear sky irradiance [Ineichen 2005a]. Figure 3.7 illustrates the diurnal variation for a single day. The deviation in the evening is caused by changes in the atmospheric parameters during the day, that are assumed constant by SOLIS.

The third step is to compare SOLIS results with ground measurements for clear sky days. Together with seven other clear sky models, SOLIS has been validated, over 16 data banks with various latitudes, altitudes and climates [Ineichen 2005a].

An upper limit of the accuracy was established by using ground measured atmospheric data as input. The SOLIS clearsky model gave a RMSE of 4% and a MBE of 2% in the horizontal global irradiance. Differences between the eight models were small, but SOLIS performed slightly better than the other models.

The use of climatic data banks instead of locally measured parameters lead to systematic underestimation of both beam and global radiation components. The standard deviation increased up to a factor two. This confirms the need for near real time atmospheric data.

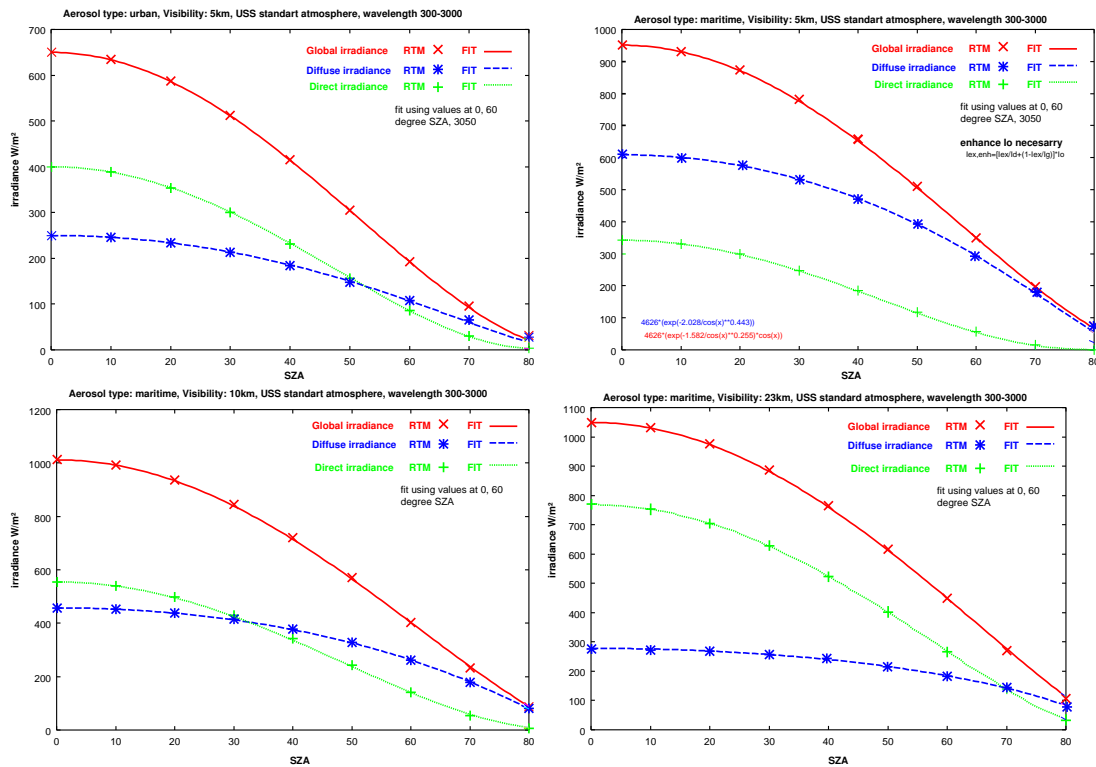


Figure 3.6: Comparison between RTM calculations and fit using the modified Lambert-Beer relation, for different atmospheric states. Points indicate the results of RTM calculations, lines indicate values calculated from with the MLB functions.

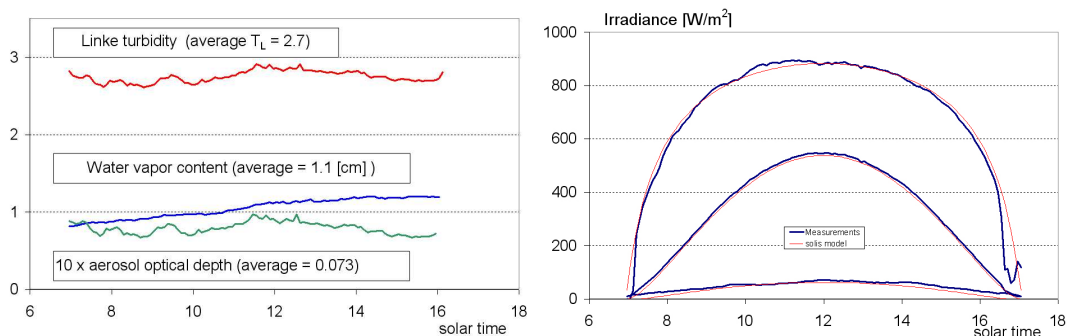


Figure 3.7: February 14, 2002, Eugene (OR). On the left graph, the stability of the atmospheric parameters is illustrated versus solar time. On the right graph, the normal beam, global and diffuse irradiance, measurements and model.

3.7 Adaptation and improvement of the existing Cloud Index method (WP 3020)

3.7.1 Adaptation of the cloud index method to MSG

A first step towards the implementation of the Heliosat-3 procedures has been the adaption of the “old” Heliosat-1 software [Kato et al., 1999] to the data of Meteosat-8 in VCS/XPIF format. The development was focused on the high resolution data in the visible range of wavelength (HRV channel) with $1 * 1 km^2$ spatial and 15 minutes temporal resolution. The software code was modified in the way that it is able to process 2 byte data for each pixel, to read and use the header information of each image, and to write all generated images with similar headers.

It was found that the VCS/XPIF data were both, shifted and distorted. A proper geolocation of Europe and the Canary Islands was made by using the software *IDRISI/Kilimanjaro* and its internal maps. This investigation revealed that an individual geolocation of many sites is necessary and that it is possible to correct for them by modifying line- and column-offsets. Therefore the new program includes options for additional offsets to recorrect the local geolocation and according site lists has been generated [Kuhlemann et al., 2005].

Later it was found that the detected distortions are a specific property of the VCS/XPIF data, while the original HRIT data contain only a few shifted images. Consequently, the switch of the whole data processing chain to these HRIT data is planned.

A proper colocation (spatial match) of sequential images has been found to be necessary as well. The old backshift procedure, developed within the European project *SoDa*, which works with a minimisation of the *rRMSE* between a test and a reference image, revealed as not satisfying. In the future, this procedure will be replaced by recommended algorithms, which uses landmarks and the correlation coefficient to detect and correct for shifted images.

With a proper data base of the described type it has been possible to optimise the different parameters of the Heliosat-1 procedure. The first step is the determination of the radiometer offset C_R for the different visible channels. It was found to be the same for all three channels ($C_R = 51$).

The second step is to determine the maximum cloud reflectivity ρ_{cloud} . According to its optimisation within the *SoDa* project it should be defined in the way that 96% of all counts are below this value [Hammer et al., 2001]. The resulting value for the HRV channel of Meteosat-8 has been $\rho_{cloud} = 650$.

To extend the angular validity of the procedure to large sun zenith angles a new atmospheric correction was developed for all visible channels. To get the whole range for all three angles (sun zenith angle, satellite zenith angle, sun satellite angle) subsets of the equatorial region and southern Africa were added to those of Europe and the Canary Islands. The derived functional dependencies have been included in the computer code. Calculated global irradiances have been compared with ground measured data

for Vaulx-en-Velin in April, May, and June 2004 as well as such calculations without an atmospheric correction. It was found that the quality is not improved by using an atmospheric correction and therefore it was omitted, because the calculation speed is much lower when using it.

The *cloud index* (n) is determined by

$$n = \frac{\rho - \rho_{ground}}{\rho_{cloud} - \rho_{ground}} \quad (3.6)$$

and the necessary ground albedo ρ_{ground} is generated using the frequency distribution of the grey counts of a monthly slot. σ_{ground} represents the half width of the land peak in the distribution and has to be optimised. This optimisation has been tried by a similar irradiance comparison like described above. The *RMSE* remained stable with varying σ_{ground} , but the *bias* increased with increasing σ_{ground} . The minimisation of the *bias* ended up with such different values for the three months, that this “mathematical” optimisation failed. Therefore, a visible determination of σ_{ground} has been applied and ended up with an value of $\sigma_{ground} = 23$. For such an optimisation the amount of cloud rests should be as small as possible, but the iteration should not collapse in the way of producing a significant amount of “dark pixels”.

Further validations for other sites in Europe and on the Canary Islands for all available HRV data (March 2004 - now) are ongoing.

This work has been described in more detail in [Kuhlemann et al., 2005] and [Kuhlemann and Hammer, 2005].

3.7.2 Development of an alternative cloud index algorithm

The cloud index is an important component of the Heliosat algorithm, which estimates solar radiation components from images of the Meteosat HRV channel. The cloud index quantifies the reflective properties of the atmosphere, and varies from 0 at clear conditions to 1 at overcast. The algorithm is semi-empirical in the way that it includes several constants that need to be tuned. Some of these were removed in the Heliosat-II algorithm [Rigollier et al., 2004] which introduced the Meteosat calibration constant to replace the “pseudo reflectivity” with a “real reflectivity”. This approach is followed here, and two additional changes are made: 1) An analytical expression is introduced to correct for backscattered radiation from air molecules. 2) A correction is made for non-lambertian reflectivity, removing the time consuming need for determining the ground reflectivity for each month and each slot.

Calculation of the reflectivity from Meteosat counts

A part of the signal that a “visible” satellite sensor receives when viewing earth is directly scattered from air molecules. This part depends strongly on the sun-ground-satellite geometry, and as the radiation at ground is independent of the satellite position, it should be corrected for. The traditional approach in the Heliosat algorithm is to

subtract a quantity from an expression which is tuned to satellite counts from cloud free pixels over sea [Hammer, 2000]. It was however shown by [Dagestad, 2001] that most of this signal is first order scattered radiance, and hence an analytical expression for this component could be used. Under the assumption of a plane-parallel atmosphere the following expression for radiance scattered towards a satellite is derived [Dagestad and Olseth, 2005]:

$$r_{atm} = I_o \frac{3(\cos^2\psi)}{16\pi} \frac{\cos\theta}{\cos\phi + \cos\theta} [1 - e^{-\tau(\frac{1}{\cos\phi} + \frac{1}{\cos\theta})}] \quad (3.7)$$

where: θ is the solar zenith angle, ϕ is the satellite zenith angle and ψ is the "co-scattering angle". I_o is the solar constant of 1367 W/m². According to the Appendix of [Dagestad and Olseth, 2005] an optical depth τ of 0.0426 is representative for the Meteosat-7 and 8 HRV channels, corresponding to an "equivalent wavelength" of 680 nanometer.

Equation 3.7 is singular for θ or ϕ at 90 degrees, but should have sufficient accuracy up to at least 85° for a spherical atmosphere. The advantage of this expression compared to the one from [Hammer, 2000] is that it is not fitted to certain angular configurations, and that it contains no signal from the surface or other atmospheric components. The reflectivity is then calculated by:

$$\rho = \frac{\pi(C - C_{off})c_f}{\epsilon I_\mu \cos\theta} - \frac{\pi r_{atm}}{I_o \cos\theta} \quad (3.8)$$

where:

- C is the raw Meteosat HRV counts
- C_{off} is the constant instrument offset (51 for Meteosat-8)
- $c_f = 0.56 \frac{W}{m^2 \cdot \mu m \cdot counts \cdot str}$ is the calibration constant
- $I_\mu = 1403 \frac{W}{m^2 \cdot \mu m}$ is the band solar irradiance of the Meteosat-8 HRV channel [Govaerts and Clerici, 2004]
- ϵ is the correction for varying sun-earth distance

The factor π is included to convert the reflected radiance to irradiance under the assumption of lambertian reflectance. This assumption is discussed in the next section. For the calculation of the cloud index ρ could be interpreted as the reflectivity of the ground and clouds, although this is not strictly physical correct.

Calculation of the cloud index from the reflectivity

In the Satel-Light version of the Heliosat scheme [Fontoynt, 1998] the (pseudo) ground reflectivity is determined for each pixel and for each month and slot. It is however seen that the reflectivity depends strongly on the co-scattering angle ψ , and thus a parameterisation will be made to correct for this.

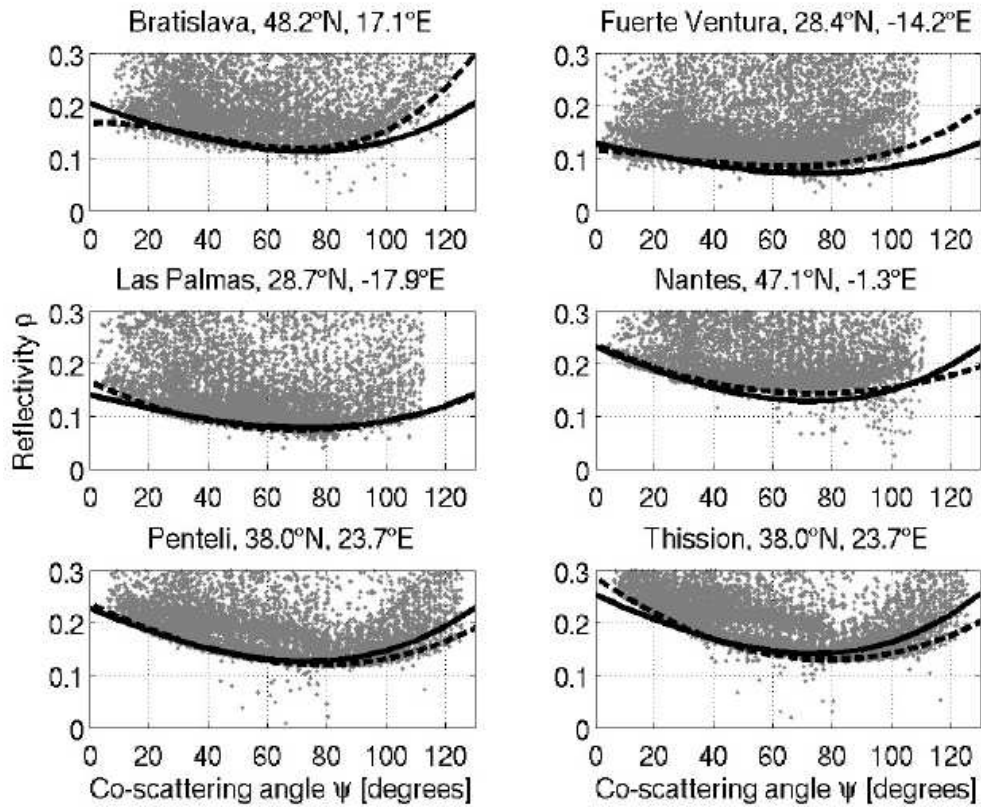


Figure 3.8: Reflectivities for the Meteosat-8 pixels of 6 European sites (dots) calculated with Equation 3.8 for all Meteosat-8 images between 16 March and 31 August 2004, plotted as a function of the co-scattering angle ψ . Broken lines: third order polynomials of ψ fitted to 4 percentiles within each ten degree bin (0-10, 10-20, etc). Solid lines: ground albedo calculated by Equation 3.10 by use of the procedure described in section 3.7.2

Figure 3.7.2 shows the reflectivity according to Equation 3.8 plotted versus ψ for six sites in Europe and the Canary Islands. For each of these sites the 4-percentile value is calculated for ψ within each ten degree bin. A third order polynomial is then fitted to these points, and plotted as broken curves on the figure. The mean of the polynomials is taken, and normalised to the value 1 for $\psi = 0^\circ$, to be used as a "shape function":

$$\rho_{gshape}(\psi) = 1 - 0.59\psi + 0.11\psi^2 + 0.05\psi^3 \quad (3.9)$$

where ψ is given in radians. The ground reflectivity can then be estimated by:

$$\rho_{ground}(\psi) = \rho_{g0}\rho_{gshape}(\psi) \quad (3.10)$$

where ρ_{g0} is the reflectivity of the pixel for $\psi = 0$. This constant is determined by taking the 4- percentile of a time series of reflectivities divided by the "shape function". To avoid noise ψ should be kept below 50° . The advantage of this approach is that the ground reflectivity can be determined once and for all, saving a lot of computer power. Besides, the difficulty of determining the reflectivity for months/slots with few clear situations is also avoided. ρ_{ground} from Equation 3.10 is plotted as solid lines on Figure 3.7.2. Still the ground albedo can be determined more frequently to account for effects which are truly due to changes of the reflecting properties of the ground surface (e.g. snow cover and vegetative changes).

The upper boundary of reflectivities (cloud reflectivity) is seen to vary much less with ψ (or solar zenith angle θ) and a constant value of 0.81 is chosen as ρ_{cloud} , taken as the 98 percentile of the counts. This is assumed to be the reflectivity of the "thickest clouds".

The cloud index is than determined with Equation 3.6.

Validation and conclusions

The new cloud index algorithm, combined with the n-k relationship [Rigollier et al., 2004] and the SOLIS clear sky model, was applied to MSG-hrv data to calculate hourly global irradiance. Table 3.2 compares the results of the new approach are compared with the operational Heliosat-3 method including the usual approach to the cloud index as described in Section 3.7.1. It can be seen that the accuracy of both methods is comparable. However, an advantage of the new alternative algorithm requires significantly less calculation time. Furthermore, it is likely that in the existing method some errors cancel out.

A more detailed validation and analysis including a separate validation of the new ground reflectivity scheme can be found in [Dagestad and Olseth, 2005]

Table 3.2: Root Mean Square Deviation (RMSD) and Mean Bias Deviation (MBD, model-observation) for the new cloud index [Dagestad and Olseth, 2005] and the existing cloud index [Hammer et al., 2003]. The reference data are hourly measurements of global irradiances for the period 16 March to 31 August 2004 . All measurements are carried out with Kipp & Zonen pyranometers, and the data are manually quality controlled by the respective data providers.

Station	Number of hours	Mean Observed [W/m ²]	New alternative cloud index		existing (Sunsat) cloud index	
			RMSD	MBD	RMSD	MBD
Barcelona	531	1475	14.7	-6.4	13.7	-3.9
Bergen	280	2073	23.4	0.2	23.1	0.0
Freiburg	389	1753	17.1	-6.0	16.5	-3.3
Geneva	459	1656	14.0	-3.1	13.8	-0.6
Lyon	432	2003	13.1	0.4	13.6	2.5
All stations	410	8960	16.1	-3.0	15.7	-1.0

3.7.3 Correction for cloud shades

The MSG hrv images revealed a large number of dark pixels. It was found, that the physical reason for these dark pixels are shades, especially cloud shades. In contrast to Meteosat-7 the data of Meteosat-8 (HRV) is strongly contaminated with such effects due to their higher spatial resolution of 1 km * 1 km (Nadir).

To get around with this problem within the cloudy sky module a modified ground albedo algorithm was developed. It takes the increment of the ground albedo iteration into account. Assuming that the sequence of iterative steps is a monotone falling function without shade contamination, an increasing increment detects shades by a sudden increase of the step width. This type of detection avoids the input of fixed thresholds between ground and shade reflectances which would not be valid for all places and times. To maintain the process a new parameter σ_S is introduced, which gives the necessary enlargement of the increment. After the detection of a shade, the according grey value is suspended from the sequence and the iteration starts again.

As shade looks like a very dark clear sky situation, although it is a cloudy sky, the next step is the construction of a sensible *cloud index* value for these cases. This is done in the way of a reconstruction by taking advantage of the used clear sky model, which is defined by Fontoynt [Fontoynt, 1998] here. Such a model determines a *clear sky index* for a given *cloud index*. Therefore, a shade value gives an according *clear sky index* and allows the assignment of a corresponding *cloud index*. Such a reconstruction conserves the statistical properties of the whole procedure.

A comparison of calculated global irradiances with ground measured data should allow the optimisation of both parameters σ_{ground} and σ_S . First results for Vaulx-en-Velin between March 2004 and January 2005 show that the opportunity to reduce

σ_{ground} improves the procedure significantly ($\Delta RMSE > 1\%$). Unfortunately, the best results are generated with values of $\sigma_{ground} = \sigma_S = 1$. This means, that the procedure iterates the lowest available ground value beside clouds and shades. It seems, that systematic errors caused by a fixed value of ρ_{cloud} are compensated under these circumstances. Such an effect is found by E. Lorenz within the ESA project ENVISOLAR.

This work has been described in more detail in [Kuhlemann and Hammer, 2005].

3.7.4 Variability correction for cloud index method

The existing Heliosat methods assume an isotropic cloud reflection. Consequently, the rRMSE for heterogeneous cloud situations can be twice as high as for homogeneous cloud situations [Hammer, 2000].

As part of the Heliosat-3 project the RTM model SHDOM was used to investigate the influence of three dimensional cloud effects on the accuracy of the Heliosat-method [Girodo, 2003, Girodo et al., 2005]. Resulting from this study a correction to the clear sky index was proposed that depends on the spatial variability of the cloud index. Such a correction is based upon the notion that the variability of clouds on pixel level is correlated with the variability on subpixel level.

This concept was further developed as part of the PVSAT2 project [Lorenz, 2004], and resulted in the following correction of the clear sky index:

$$k_{corrected}^* = k_{old}^* - bias_{\alpha}(k_{old}^*, var) \quad (3.11)$$

where:

$k_{corrected}^*$ is the corrected clear sky index.

k_{old}^* is the 'old' clear sky index as defined by equation 3.6.

$$\begin{aligned} bias_{\alpha}(k_{old}^*, var) = & a_{\alpha,0} + a_{\alpha,1}k_{old}^* + a_{\alpha,2}var + a_{\alpha,3}k_{old}^{*2} + a_{\alpha,4}k_{old}^*var \\ & + a_{\alpha,5}var^2 + a_{\alpha,6}k_{old}^{*3} + a_{\alpha,7}k_{old}^{*2}var + a_{\alpha,8}k_{old}^*var^2 \\ & + a_{\alpha,9}var^3 + a_{\alpha,10}k_{old}^{*2}var^2 \end{aligned} \quad (3.12)$$

α indicates a class of solar zenith angle, three classes have been defined.

var is a measure of the spatial variability and defined by:

$$var = \frac{1}{N} \sum_{i,j} ((n_{i,j} - n_{i,j-1})^2 + (n_{i,j} - n_{i-1,j})^2) \quad (3.13)$$

For Meteosat7 based data this method gave a considerable improvement of the bias for winter months.

In the Heliosat-3 project a first test of this approach was carried out by applying the above correction, as is, to MSG based data. No significant improvement was observed. However, due to the smaller pixelsize of MSG data it is to be expected that

the parameters $a\alpha, x$ will need to be determined separately for an MSG based scheme. This will be carried out as part of the vIEM project.

3.8 New COD based cloudy sky scheme: CloudS (WP 3020)

3.8.1 Development

To derive a new “all sky” scheme for radiative transfer within the Heliosat-3 project, a new “cloudy sky” scheme has been developed. The goal of this work is the replacement of *Cloud Index* based calculation schemes like the Heliosat-1 procedure.

The new “cloudy sky” scheme CloudS modifies the “clear sky” irradiance given by SOLIS (Section 3.6) and uses information about clouds provided by the APOLLO procedure. APOLLO has been developed at DLR (Section 3.2) and its products contain the optical depth τ_c , the cloud fraction, three different altitudes, two different cloud types and in the future probably effective droplet radii r_{eff} of clouds. These data are calculated from several visible and infrared channels and have a spatial resolution of 3 km * 3 km (Nadir), if APOLLO is applied to Meteosat-8.

While RTM’s are too slow for operational use, these models are used for parameterisation of radiative transfer. Here, the investigations were done by using the radiative transfer software SBDART, which allows the simulation of total overcast situations. After sensitivity studies of the effects of cloud altitude and thickness on irradiance at ground level, the wavelength dependence of such effects was studied.

Finally, it was decided to parameterise the radiative transfer through clouds for all Kato-bands (wavelength dependence) with a representative cloud from 1 km to 2 km height.

An atmospheric profile for *Midlatitude Winter* was chosen, not to have too strong water vapour effects. Furthermore, the atmosphere has been aerosol-free to ensure the general applicability of the results. An isotropic ground reflecting model for vegetation has been chosen within SBDART, because it is the closest to sites of measurement. An implicit construction of the following type has been used to parameterise radiative transfer through clouds with properties τ_c, r_{eff} , and with varying solar zenith angle Θ :

$$\frac{I_{SBDART}^{Cloudy}}{I_{SBDART}^{Clearsky}} = f(\tau_c(\Theta(r_{eff}))); \quad \tau_c \in [0; 300]; \Theta \in [0 : 80]; r_{eff} \in [6 : 50] \quad (3.14)$$

Commonly used radiative transfer relationships have not been successful when applied. A screening of numerous functional relationships finally resulted in the following set of equations:

$$f(\tau_c) = \frac{a_1}{1 + a_2 * \tau_c}; \quad (3.15)$$

$$a_1 = a_1(\Theta) = a_{11} - a_{12} * \Theta^{a_{13}}; \quad (3.16)$$

$$a_2 = a_2(\Theta) = a_{21} + a_{22} * \Theta^{a_{23}}; \quad (3.17)$$

$$a_{j1} = a_{j1}(r_{eff}) = \frac{a_{j11} * r_{eff}}{a_{j12} + r_{eff}} + a_{j13} * r_{eff}; \quad j \in (1, 2); \quad (3.18)$$

$$a_{j2} = a_{j2}(r_{eff}) = a_{j21} * (1 + r_{eff})^{a_{j22}}; \quad j \in (1, 2); \quad (3.19)$$

$$a_{j3} = a_{j3}(r_{eff}) = a_{j31} * (1 + r_{eff})^{a_{j32}}; \quad j \in (1, 2) \quad (3.20)$$

The resulting parameterisation gives 14 coefficients a_{jik} for each Kato-band [Kato et al., 1999] (4-29 corresponding to wavelength $\lambda \in [307 \text{ nm}, 3002 \text{ nm}]$).

3.8.2 Validation

To get a first idea of the quality the whole target space has been calculated with the new parameterisation CloudS and compared with the original SBDART results. There are two complicated situations. For very small optical depth and small solar zenith angles the intensity does not decrease compared to the “clear sky” case, but the parameterisation is not able to reproduce this. Secondly, for large optical depth (and small irradiance) deviations between SBDART and CloudS increase steadily.

In a second validation step APOLLO (adapted to Meteosat-8) derived properties of clouds have been used for Vaulx-en-Velin. Because of the boundary conditions of SBDART only situations with cloud fractions 1 - total overcast - are used. For comparison direct calculations with the *libRadtran* software have been done. *libRadtran* uses the SBDART solver as well, but within *libRadtran* it is possible to define aerosol and water vapour content individually, and this has been done with climatological values for Vaulx-en-Velin. Therefore, the *libRadtran* results set an upper limit to the accuracy, achievable with CloudS.

Finally, the accuracy of the SOLIS scheme using the *Cloud Index* part of the old Heliosat-1 procedure is given to evaluate the overall quality. A typical diurnal variation of irradiance measured and calculated with three methods is given in Figure 3.9. The figure illustrates that the quality of the *libRadtran* calculations using APOLLO products as input does not match that of the SOLIS/Cloud index scheme, but reveals a positive bias. Therefore it would be of interest to investigate, whether this belongs to the boundary conditions used within *libRadtran* or to the quality of the cloud information, provided by APOLLO. A second result is, that the quality of the new parameterisation CloudS shows an additional bias. A detailed investigation of the reasons reveals, that this does not belong to the ideal, unrealistic description of the atmosphere - a lack of many scatterers - and the “wrong” ground reflection, but to the inaccuracies of the functions used to parameterise. However, it is necessary to validate CloudS with other sites of measurement and for all seasons, to get a closer look.

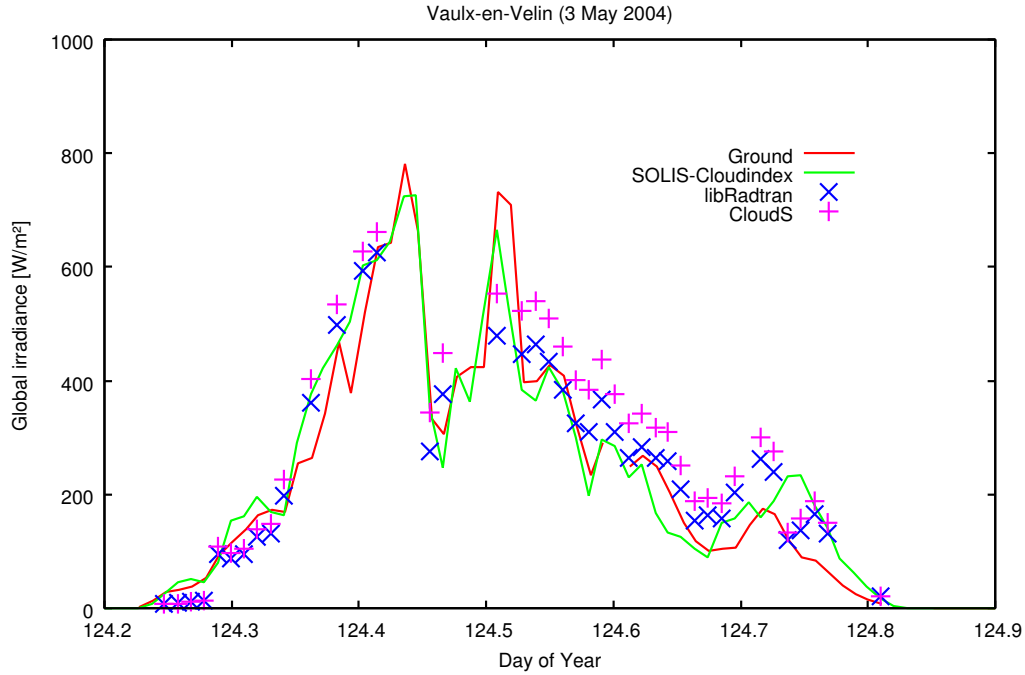


Figure 3.9: Example (of good quality) for the diurnal variations of the global irradiance in Vaulx-en-Velin on May 3rd. Calculations using APOLLO products (*libRadtran*, *CloudS*) were done only for total overcast situations. For comparison ground measured data and *SOLIS/Cloud index* results are given.

To get quantitative information about the quality of all methods used, a statistical comparison is given in Table 3.3. It presents the *RMSE* and the *bias* for comparisons between the 3 methods and the ground measured data for the months March - August. The table shows comparably small deviations between *CloudS* and *libRadtran*, while the deviations from ground measured data are significantly larger.

To improve the quality of *CloudS*, a different function for parameterisation ($f(\tau_c) = (a_1 + a_2 * \tau_c)^{a_3}$) would allow a more accurate description. To reduce the necessary number of coefficients it is possible to omit the variable r_{eff} , at least as long as this APOLLO product is not available. For this case a mean value of $r_{eff} = 8\mu m$ can be used. After such a reduction of the problem it might be also possible to test functional compositions $f(\tau_c) = f_1(\tau_c) + f_2(\tau_c)$, which would probably solve the complicated situation for low optical depths (< 5).

To get a new “all sky” scheme, it is necessary to investigate the handling of the APOLLO product “cloud fraction” and related to that, the situation for broken cloud situations. Finally, the quality of APOLLO products in general is to be investigated. Fortunately, it is already on the way within the ESA project *ENVISOLAR* and the Virtual Institute Energy Meteorology (*vIEM*).

Table 3.3: Intercomparison between 3 different methods to derive global irradiances in total overcast situations. Calculated results are compared with ground measured data (Ground) for Vaulx-en-Velin for April to August 2004. Monthly averages of data with 15 minutes time resolution are given. libRadtran (Lib) and Parameterisation (CloudS) values are calculated with a standard water cloud between 1 km and 2 km height, effective droplet radii of 8 μm , and the optical depth τ_c derived from Meteosat-8 with APOLLO. For evaluation the errors of the SOLIS/Cloud index (SO/Cl) method are given as well. It should be noted that the SOLIS/Cloud index scheme uses HRV data which have a higher spatial resolution as the channels used for the APOLLO/libRadtran scheme.

Comparison	Error	March	April	May	June	July	August
SO/Cl - Ground	<i>RMSE</i> (%)	44.44	47.72	40.75	36.64	50.16	46.24
SO/Cl - Ground	<i>bias</i> (%)	0.75	12.76	10.93	1.16	-1.65	4.25
Lib - Ground	<i>RMSE</i> (%)	55.70	65.15	55.55	49.58	80.57	74.83
Lib - Ground	<i>bias</i> (%)	24.76	23.35	11.68	6.95	13.02	14.24
CloudS - Ground	<i>RMSE</i> (%)	64.05	80.32	65.48	54.66	81.23	76.02
CloudS - Ground	<i>bias</i> (%)	35.57	44.03	28.44	20.18	23.20	24.74
CloudS - Lib	<i>RMSE</i> (%)	11.89	20.80	19.49	17.39	14.16	14.02
CloudS - Lib	<i>bias</i> (%)	8.67	16.76	15.01	12.37	9.00	9.18
Total overcast cases		313	595	498	427	267	428

3.9 The all weather module (WP 3020 / 3030)

The actual irradiance is calculated from the MLB-parameters from the SOLIS clear sky module and cloud index images provided by any of the cloud modules are combined in the all weather module n2irr. n2irr is based on the module cloud index2G from the Heliosat-1 procedure.

3.9.1 Technical adaptations

The n2irr module can work with Meteosat-7 as well as MSG data. To allow this technical adaptations were necessary to deal with: different header formats, different spatial and temporal resolution and different file formats.

3.9.2 Direct and diffuse irradiance (WP 3030)

In Heliosat-1 the direct and diffuse irradiance are derived using the Skartveith Olseth method [Skartveit et al., 1998] that uses the clear sky irradiance and the extra terrestrial irradiance as input. The SOLIS clear sky module provides the additional information of the clear sky direct irradiance. Consequently it has been possible to develop a new method to derive the (all weather) direct irradiance [EHF et al., 2003]

$$I_{dir} = I_{dir,clear} * (k - A * (1 - k))^b \quad (3.21)$$

where k is the clear sky index and A and b are empirical parameters.

The diffuse irradiance can then easily be derived by subtracting the direct irradiance from the global irradiance.

3.9.3 Spectrally resolved all weather irradiance (WP3040)

Scattering of light against cloud particles changes the spectral distribution of irradiance under clouds compared to the clear sky irradiance. The current operational version of the cloud module gives only a wavelength independent cloud index value. A correction to the clear sky irradiance spectral distribution for cloudy situations, in the form of look-up tables, has been developed using the RTM model libRadtran [Mayer and Kylling, 2005].

3.10 Angular distribution (WP3030)

An important input of ray tracing models used in architecture is the sky luminance distribution. This parameter is not routinely acquired, even if it is recommended by the CIE. A modelisation of the sky vault luminance distribution based on a radiative transfer models is not feasible with the actual input parameters. An attempt was conducted

in Geneva to correlate the a-symmetry of a real sky distribution with 41x41 pixels satellite images, but without significant results. Existing symmetric sky luminance distribution models are evaluated in the present work, and recommendations are given for the use of them. In the present context and taking into account the small quantity of data and input parameters, it was not possible to increase the accuracy of the sky luminance distribution models. A performance comparison was conducted on a 10 weeks measurements period for 9 models that confirm previously published validations. Two models are slightly better, the ASRC-CIE and the Perez Model. The first is a discrete model based on look-up Angular distribution of the diffuse illuminance 2005 tables, the second is a mathematically continuous model [Ineichen, 2005b]. All the models use irradiance or illuminance components as input parameters. The conclusion of the present study is that the indirect way (i.e evaluation of the sky luminance distribution on the basis of irradiance and/or illuminance parameters) still gives the best results, even if the sky distribution can only be symmetrically modelled. The modelled luminances are normalised by the diffuse illuminance; it is therefore important to have access to good quality input parameters.

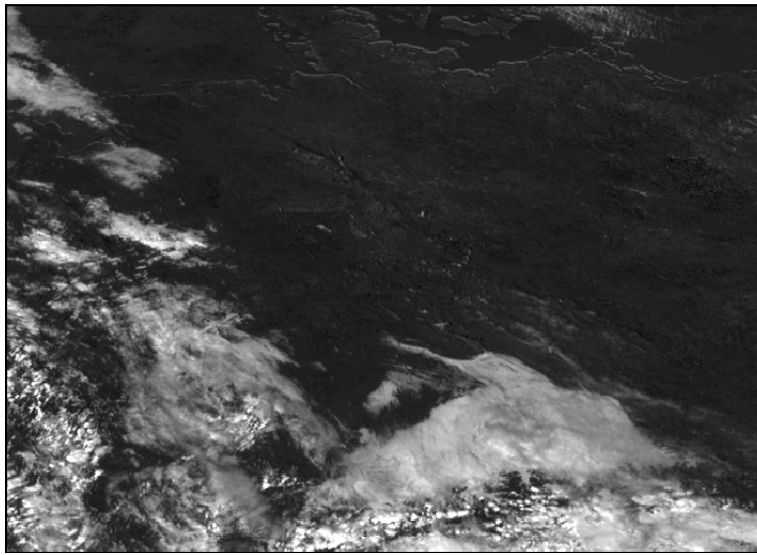
3.11 Spatial irradiance structure (WP 3050)

3.11.1 Measures for the local spatial variability of the irradiance field

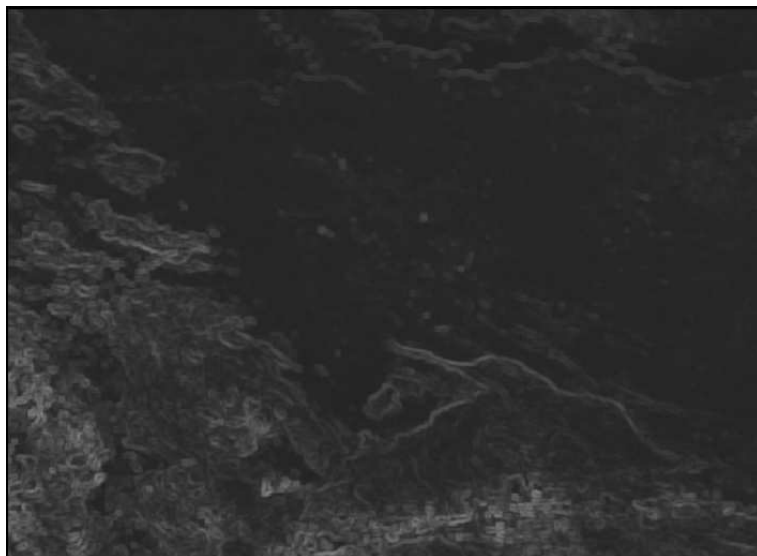
A measure for the local variability of the cloud index is required for the variability correction of the cloud index method (Section 3.7.4), as well as for the split of global irradiance into its diffuse and direct components. Two variability measures are currently in use, the standard deviation of the data within a 5x5 block of pixels and the variability index defined in Equation 3.13. The measures are not identical, it is therefore of interest to investigate their correlation in view of a possible interchange in the procedures using the measure.

This study a 10-day sample of cloud index images with a section of 660×480 Meteosat8 pixels covering Germany is analysed. Examples of a cloud index image, a local standard deviation image and a variability index image can be found in Figure 3.10. As may be noticed, the visual appearance of the two variability maps is quite similar. A quantitative analysis results in a cross correlation coefficient of 0.96 for this pair of images. Repeating this analysis for the 12:15 clear sky index images for all 10 days analysed gives an average cross correlation coefficient of 0.94.

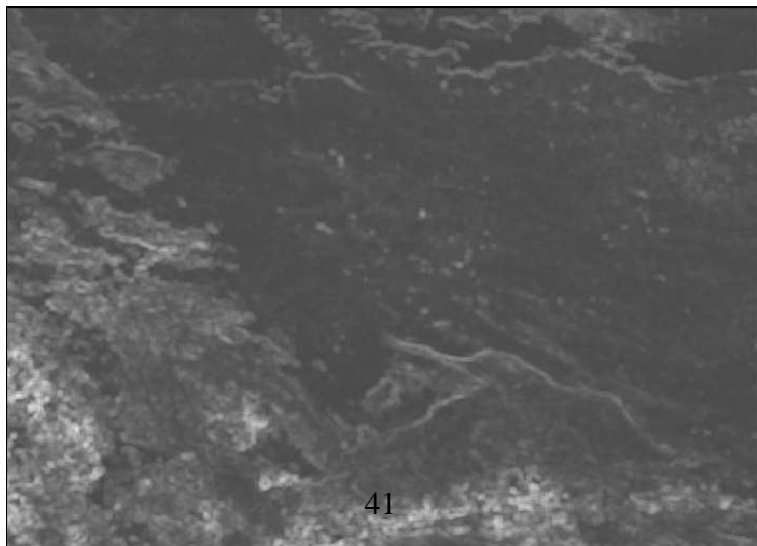
The analysis reveals that the measures 'local standard deviation' and 'variability index' mainly render the same information for the cloud index images analysed. Thus it may be expected, that the procedures using these measures, the variability correction of the n-kt* relation and the split of the global radiation to its direct and diffuse components may as well be based on a unique measure.



(a) Cloud index



(b) Cloud local standard deviation



(c) Cloud variability index

Figure 3.10: *Cloud index and cloud index variability, October 12th 2004, 12h15.*

3.11.2 Spatial statistics of irradiance data

The knowledge of the spatial structure is of importance for both, the merging of satellite and ground station data to gain optimal knowledge and the application of solar irradiance data for applications that involve networks i.e. spatially distributed structures. Treating these topics, the representation of the spatial cross-statistics of the irradiance field as expressed by the cross-correlation function or the variogram play an important role.

Data from the network of ground stations installed on the Canary Island and the Heliosat3 derived irradiance data for respective pixels are used to compare the satellite derived cross-statistics with their ground station derived counterparts. For the present study 15min averages of radiation data from 8 stations located on the Islands of Fuerteventura (3 stations), Gomera, El Hierro, Lanzarote (1 station each) and Tenerife (2 Stations) for the month of December 2004 have been selected.

An analysis of single point data shows that the satellite data underestimates the variance of the ground data on the 15 minute timescale.

The correlation of the clear sky indices at two different locations can be expressed with *cross correlation coefficients* (see [Beyer et al., 2005]). Cross correlation coefficients calculated from satellite data in good agreement with coefficients calculated from ground data.

As a second measure for the spatial structure of the clear sky index fields, the average squared difference of the clear sky index is inspected. This measure is selected due to its importance in calculating the variogram of the field. When applied to satellite data the results show a significant underestimation compared to ground data. This is due to the variance underestimation noted above. After normalisation with the variance the agreement improves and a correlation coefficient of 0.84 between satellite and ground data is obtained.

Based on the example analysed it may be concluded that the basic spatial structure i.e. the co-occurrence of positive and negative deviations from the mean at two locations is well represented by the Meteosat8 based Heliosat3 data. As a shortcoming, it has to be stated that the satellite derived data are not able to cope with the variability of the 15 minute means of the ground data. Even with the improved spatial resolution of the Meteosat8 images the dynamics of the satellite derived irradiance field are reduced. It may however be expected that based on a higher number of ground data sets a correction procedure for the satellite derived variability measured could be identified.

A more detailed description of this work can be found in [Beyer et al., 2005].

3.12 Solar Energy processing Chain (WP 4010)

Aim of WP 4010 was to implement test and begin a routine processing chain for solar energy specific data. In practice the work consisted of the following steps:

1. Installation of hardware and software for the reception of MSG data at Oldenburg University.
2. Setup of a back-up mechanism for MSG images in co-ordination with DLR.
3. Adaptation of the existing Heliosat-1 software and processing chain for the use of MSG data.
4. Adaptation of the new Heliosat-3 software and processing chain for the use of MSG data.
5. Further automation of the Heliosat-3 software as developed in WP 3000.
6. Adaptation of the Heliosat-3 software
7. Setup of a semi-automated data exchange to facilitate the validation of the Heliosat-3 procedure

The adaptation of the existing Heliosat-1 software is described in detail in Section 3.7. The validation of the Heliosat-3 method had a large similarity with the normal operation of the solar energy processing chain: It required the production of large quantities of irradiance data for several locations and the exchange of this data with the project partners via the projects webserver. The datasets needed to be updated regularly due to new improvements to the software and the availability of new MSG-data.

The components "katoshell" and "n2irr" from the working version of the Heliosat-3 software (deliverables D8.1 and D8.2) were designed to calculate short time series for a single point. To facilitate the validation of the Heliosat-3 procedure and future implementation in the day-to-day operation, the software was adapted so that irradiance values could be calculated for several locations and an arbitrary long time period. The upload of the data to the webserver was also semi-automated.

Furthermore, work packages 3050 WP 3050 (Spatial irradiance structure) and WP 6020 (Solar Thermal Power Plants) needed irradiance and variability maps. Therefore, a separate version of the Heliosat-3 software was developed to calculate irradiance maps.

Further integration in the day to day operation of the Heliosat-3 software will take place as part of the ENVISOLAR project.

3.13 Climatological Processing Chain (WP 4020)

This WP aimed at realising, implementing and testing a chain for the routine processing of MSG data with emphasis on climate research and atmospheric applications. The major tasks were:

- integration of retrieval data and basic MSG data into processing chain,
- conditioning of the processing system (set up of look-up tables etc.)
- implement intelligent mechanisms for effective and user-friendly access to results
- definition of different product levels (primary, secondary, ..) according to customer needs
- quantify benefits of the improved/new products.

These tasks of WP 4020 are similar to those of WP 4010 but with the addition that the targeted application in WP 4020 is oriented towards long-term irradiance data with an emphasis on climatology-related topics (long-term time series, GIS, cartography). This implies the set-up of a parallel processing chain since the single steps have to be performed on different data sets, with different goals (i.e. user needs) and under different time constraints. Actually, these tasks were not achieved in their integrality in the framework of the project Heliosat-3, mostly because of the delays in previous work packages, caused themselves by delays in satellite operations. Nevertheless, a number of activities were held that will benefit to the establishment of the climatological chain which will take place even if the project is finished. In brief, these activities were:

- construction of an hybrid chain, working in real time since February 2004
- gaining experience in MSG operation, real-time acquisition of MSG data, daily management of troubles
- testing, validating some solutions in computer system, database structure, processing speed
- testing some solutions in image processing and ground albedo management
- preparing an operational chain: design and modelling
- test exchange of data with DLR
- providing outputs of the hybrid chain to selected customers for testing

Conclusions are:

- the hybrid method can process MSG data efficiently
- it can run very fast, every 15 minutes
- the same chain can operate also off-line
- several tools have been tested and improved
- testing customers provide some feedback on products

Table 3.4: Inputs for the wavelength dependent aerosol optical depth. The Shettle typology gives a wavelength dependent AOD.

input	time scale	reference
default Shettle classification. i.e. urban, maritime, rural	half yearly	[Shettle and Fenn, 1976]
SYNAER climatology	yearly	Section 3.4
Shettle classification scaled with GACP	half yearly (Shettle) monthly (GACP)	[Mischenko et al., 2002]

Table 3.5: Input for atmospheric water vapour in the SOLIS clearsky module.

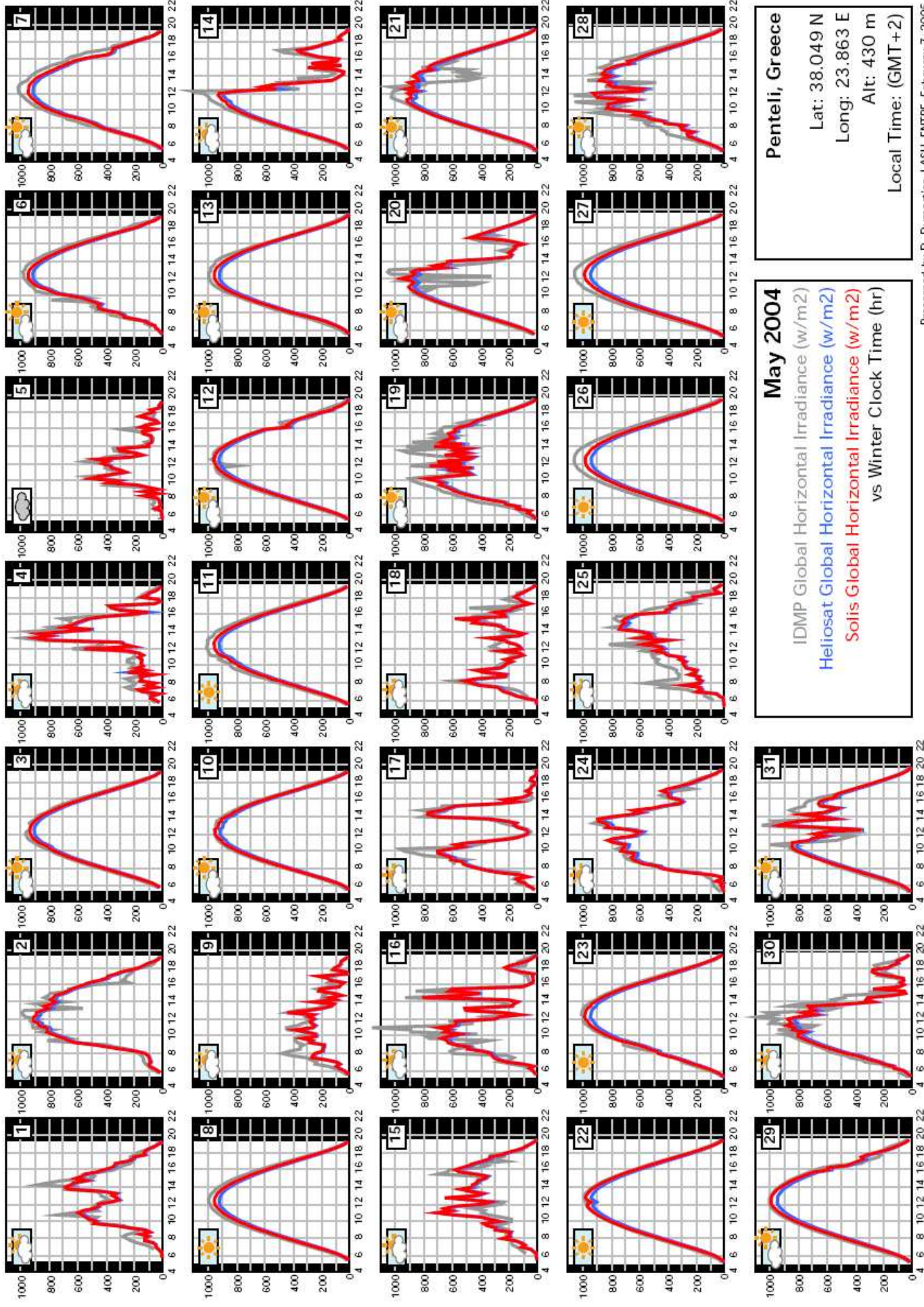
input	time scale	reference
default value 0.1	∞	-
NVAP	monthly	[Randel et al., 1996, Simpson et al., 2001]

3.14 Validation of the operational Heliosat-3 irradiance calculation scheme (WP 5020)

3.14.1 Operational Heliosat-3 irradiance scheme

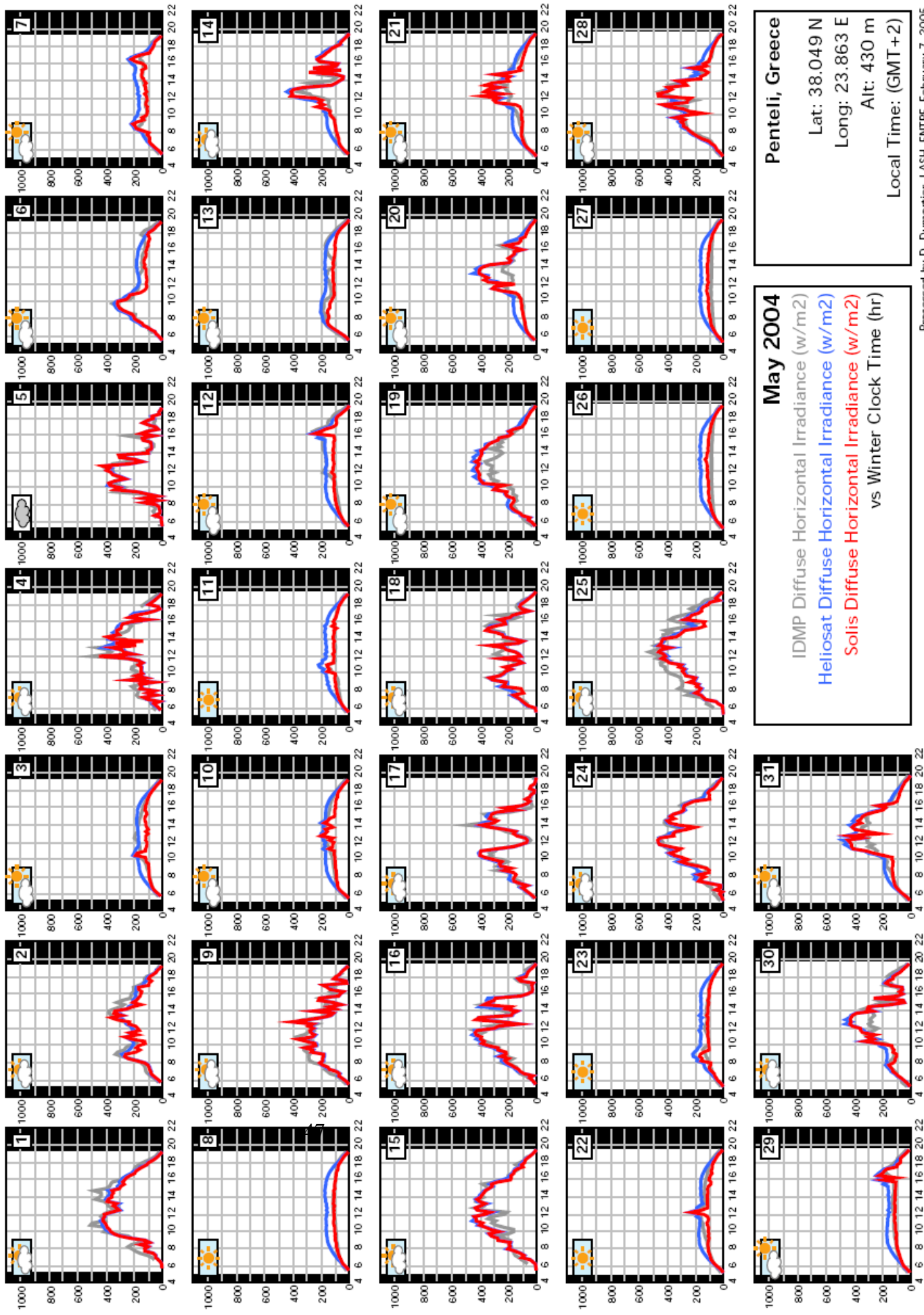
The COD based irradiance scheme is promising but could not be developed to a stage it could be included in an operational scheme (see section 3.8) within this project. As an alternative an operational scheme was developed that consists of the SOLIS clear sky module, an MSG optimised Cloud index module and the MSG adapted all-weather module (see Figure 3.1).

The SOLIS clearsky module is designed to use satellite based (near) real time atmospheric data as input (see Sections 3.3 to 3.5 and 3.6). Historic timeseries of satellite based data have been prepared for the aerosol, water vapour and ozone content of the atmosphere. However, these data were either available for only a part of the validation period, or for an earlier period. Therefore calculations were carried out with several climatological datasets of atmospheric parameters, that are described in Table 3.4 and 3.5. A default value was used for ozone, since this plays only a role in the UV region.



Penteli, Greece
 Lat: 38.049 N
 Long: 23.863 E
 Alt: 430 m
 Local Time: (GMT+2)

May 2004
 IDMP Global Horizontal Irradiance (w/m2)
 Heliosat Global Horizontal Irradiance (w/m2)
 Solis Global Horizontal Irradiance (w/m2)
 vs Winter Clock Time (hr)



Penteli, Greece
 Lat: 38.049 N
 Long: 23.863 E
 Alt: 430 m
 Local Time: (GMT+2)

May 2004
 IDMP Diffuse Horizontal Irradiance (w/m²)
 Heliosat Diffuse Horizontal Irradiance (w/m²)
 Solis Diffuse Horizontal Irradiance (w/m²)
 vs Winter Clock Time (hr)

3.14.2 Global horizontal irradiance

The global horizontal irradiance calculated was validated with pyranometer measurements from meteorological stations across Europe. Tables 3.6, 3.7 and 3.8 show the results of the validations performed at LASH-ENTPE, ITC and UiB, respectively. All of the results shown here use the same SOLIS clear sky model of aerosols from SYNAER and water vapour from NVAP.

Dumortier and Roy validated for a slightly longer time-period than Dagestad, hence the differences for Freiburg and Vaulx-en-Velin between Table 3.6 and Table 3.7.

Except for a few stations, the Mean Bias Deviation (MBD) and Root Mean Square Deviation (RMSD) are small and well within the objective of the proposal for the project. For monthly, daily and hourly values of global horizontal irradiance the aims were a RMSD of 5%, 10% and 20% respectively. Only one station is of high latitude, Bergen at 60.4 degrees north. Here a relatively large RMSD of 23.1% for hourly irradiances is found. This station also gives higher RMSD than the other stations for similar solar elevations and values of the cloud index, so this confirms the expected result that the Heliosat algorithm gives generally lower accuracy for higher satellite zenith angles. However, it is found that the frequency distribution of irradiances is as good for Bergen as for the other sites, although the hour by hour match is lower.

For the stations at the Canary Islands (Table 3.8) the MBD is generally quite large (model gives too high values), except for one station, Izaa (Teide), with an underestimation of 15%. (Note that the station is located at an elevation of 2398 meters, whereas all other stations are below 1000 meters) At many of these stations more than 60% of the situations were cloud free, and therefore it is likely that the reason of the overestimation is that the clear sky model gives too high values for the Canary Islands. (For the station at Teide the high elevation is a likely explanation for an underestimation instead). This demonstrates that the SOLIS model only shows its benefits when the input data are representative of the time and location. The consortium believes in further improvements of the results when operational retrieval of atmospheric parameters are used as input to the SOLIS model.

The figure on page 46 illustrates that the Heliosat-3 estimates reproduce the 15 minute variations of solar radiation remarkably well. This is very important for any application which depends on the dynamics of solar radiation. The finer time resolution of Meteosat-8 than previous satellites makes such estimates possible.

The validation by Knut-Frode Dagestad (Table 4) also shows a comparison against hourly global irradiances retrieved from Meteosat-7 data with the Heliosat-1 algorithm Fontoynt et al. (1998). Where the Heliosat-1 algorithm gives an overall RMSD of 18.3 percent, the Heliosat-3 algorithm using MSG data shows an improvement with an RMSD of 15.7 %.

Table 3.6: Results from the validation of global irradiances calculated with the operational Heliosat-3 method performed by Dominique Dumortier at LASH-ENTPE [Dumortier and van Roy, 2005]. The three first columns show the Root Mean Square Deviations (RMSD) given in percent of the mean observed 15 minute, daily and monthly sums respectively. The last column shows the MBD (model - observation) calculated for the 15 minute value, also given in percent of the mean observations.

Station	RMSD			MBD
	15 min	daily	monthly	15 min
Bratislava	23.3	8.5	3.8	3.8
Freiburg	22.4	6.6	2.4	-1.9
Nantes	32.2	15.8	10.8	-9.4
Vaulx-en-Velin	21.7	7.6	6.2	3.4
Penteli	17.0	7.9	7.1	-5.2
Thission	16.2	6.7	2.8	-1.9
All stations	22.1	8.9	5.5	-1.9

Table 3.7: Results from the validation of global irradiances performed by Knut-Frode Dagestad at the University of Bergen. The validation period runs from 16 March to 31 August 2004. The version of Heliosat-3 is the same as in the validation by Dominique Dumortier (Table 3.6). The Root Mean Square Deviations (RMSD) and Mean Bias Deviations (MBD, modelled observed) are given in percent of the mean observed hourly, daily and monthly values respectively.

Method Satellite	Heliosat-3 MSG				Heliosat-1 Meteosat7	
	MBD	RMSD			MBD	RMSD
Station	hourly	hourly	daily	monthly	hourly	hourly
Barcelona	-3.9	13.7	8.1	6.1	0.4	15.9
Bergen	0.0	23.1	9.6	3.0	9.3	29.1
Freiburg	-3.3	16.5	9.2	3.0	-1.4	18.5
Geneva	-0.6	13.8	8.5	3.0	0.4	15.9
Vaulx-en-Velin	2.5	13.6	8.2	2.2	1.6	14.7
All stations	-1.0	15.7	7.2	2.6	2.6	18.3

Table 3.8: Results from the validation of Heliosat-3 for 15 minute values of global irradiance performed by Antonio Ortégón Gallego at ITC. The period of validation is different from station to station and is shown in the second column. The version of Heliosat-3 is the same as in the validation by Dominique Dumortier (Table 3.6). The Root Mean Square Deviations (RMSD) and Mean Bias Deviations (MBD, modelled observed) are given in percent of the mean observed hourly, daily and monthly values respectively. Results are shown for two different clear sky models: SOLIS and the model used by the Satel-Light project [Fontoynt, 1998].

Station	Time period	Nr. of Observations	Mean Irrad. [W/m ²]	Heliosat-3		Heliosat-1	
				MBD [%]	RMSD [%]	MBD [%]	RMSD [%]
Pozo Izquierdo	Mar 04 - Jan 05	12426	510.5	4.6	15.1	6.0	15.8
Las Palmas	May 04 - Jan 05	10035	430.6	11.8	26.5	8.5	25.2
Maspalomas	May 04 - Jan 05	6988	463.2	16.2	28.2	20.7	31.0
Santa Brgida	Aug 04 - Jan 05	5943	367.2	12.9	27.3	17.1	30.2
Mogn	Aug 04 - Jan 05	5943	412.3	12.8	29.2	20.7	34.4
Betancuria	Aug 04 - Jan 05	9390	489.3	5.5	17.8	9.2	19.6
Caadas del Ro	Aug 04 - Jan 05	8701	499.1	3.9	17.6	6.9	18.7
El Cotillo	Aug 04 - Jan 05	4677	457.1	3.8	16.3	6.5	17.8
San Sebastian	Jun 04 - Dec 04	7950	518.0	6.5	16.1	10.7	18.5
Valle Gran Rey	Aug 04 - Jan 05	5872	426.9	9.8	29.7	15.3	32.2
Valverde	Aug 04 - Jan 05	8107	367.2	35.6	51.2	35.0	50.6
La Restinga	Aug 04 - Jan 05	9234	482.4	12.8	24.9	18.6	27.9
Janubio	Aug 04 - Jan 05	8460	454.8	12.8	25.0	16.9	27.6
Los Valles	Aug 04 - Jan 05	3429	468.6	10.7	21.9	8.5	21.2
Santa Cruz de LP	Sep 04 - Jan 05	4937	315.1	16.7	38.2	15.7	37.8
La Laguna	Sep 04 - Jan 05	9685	481.3	6.9	23.0	11.7	25.0
Puerto de la Cruz	Sep 04 - Jan 05	5275	421.6	0.2	29.1	3.4	30.6
Santiago del Teide	Sep 04 - Jan 05	6033	506.8	3.4	18.0	9.5	21.3
Granadilla	Aug 04 - Jan 05	4335	434.7	13.1	25.8	17.3	28.3
Izaa (Teide)	Mar 04 - Dec 04	9284	623.8	-15.5	24.1	-9.6	21.0
Average		7335	465.5	8.8	24.7	12.0	26.1

Table 3.9: Results from the validation of diffuse irradiances calculated with the operational Heliosat-3 method. Climatological values from the SYNAER and NVAP datasets have been used for aerosol and water vapour, respectively. The three first columns show the Root Mean Square Deviations (RMSD) given in percent of the mean observed 15 minute, daily and monthly sums respectively. The last column shows the Mean Bias Deviation (MBD, model - observation) calculated for the 15 minute value, also given in percent of the mean observations. Since the MBD is independent of the time-scale it is only given for 15 minute values.

Station	RMSD			MBD
	15 min	daily	monthly	15 min
Bratislava	34.3	16.3	10.1	-9.3
Freiburg	33.5	16.6	2.5	0.3
Geneva	36	-	-	-5
Nantes	39.5	18.7	8.9	-7.2
Vaulx-en-Velin	32.8	14.8	4.8	-1.4
Penteli	33.2	19.5	7.4	-5.7
Thission	32.7	16.9	1.9	-1.6
All stations	34.3	17.1	5.9	-4.2

3.14.3 Diffuse and direct Irradiance

Direct irradiance is of importance for planning, design and performance control of solar energy systems using concentrators, such as solar thermal electric systems (see Section 3.16) and concentrator photovoltaic cells. More over, it is necessary to know how the global irradiance is divided between direct and diffuse irradiance in order to calculate the irradiance on a tilted plane.

Within the operational Heliosat-3 scheme the direct irradiance is calculated with equation 3.9.2. Diffuse irradiance is calculated by subtracting this from the global irradiance. The diffuse fraction model of Olseth et al. (1998) is used by the reference Heliosat-1 method.

Table 3.9 shows the results of the validation for 7 sites in Europe.

The RMSE of the Heliosat-1 method is comparable with the Heliosat-3 method. However the MBE of the Heliosat-3 method is significantly better than the reference method.

It was found that the Heliosat-3 method this method gave better results than using the diffuse fraction model of Olseth et al. (1998) which generally overestimated diffuse irradiance. The new method also ensures consistency in that all parameters are calculated using only the cloud index and the SOLIS scheme. There are two independent validations of diffuse irradiances. Pierre Ineichen found an RMS of 36% and a MBD of -5% (model observation) for 15 minute values for the station of Geneva.

The mean RMSD and MBD for 15 minute values are similar to what is found by Pierre Ineichen; 34.3% and -4.2% respectively,

Table 3.10: Results from the validation of global and diffuse illuminance. The results are calculated using the cloud index from the University of Oldenburg and the SOLIS clear sky model with climatological values of aerosols from SYNAER and water vapour from NVAP. The illuminances are calculated from the irradiances using the luminous efficacy model of Perez and with the spectral integration of SOLIS spectral bands (global illuminance only). All numbers are given as percentages of the mean observations.

Station	Global illuminance				Diffuse illuminance	
	Perez		SOLIS		Perez	
	RMSD	MBD	RMSD	MBD	RMSD	MBD
Bratislava	23.1	5.6	26.9	12.8	33.3	4.8
Nantes	32.1	1.8	33.4	5.9	38.4	5.4
Vaulx-en-Velin	20.7	3.3	23.5	10.3	31.3	1.2
Penteli	17.4	-6.6	16.2	-0.2	-	-
Thission	17.2	-7.5	16.0	-2.9	-	-
All stations	22.1	-0.7	23.2	5.2	34.3	3.8

3.14.4 Illuminance

One of the advantages of the new Heliosat-3 scheme is that it provides spectral output. (see Sections 3.6 and [EHF et al., 2003]). Illuminance can be determined by numerically integrating the product of the spectrally resolved irradiances and a sensitivity of the eye filter.

Comparing with observed illuminance, it was found that this method gave best results for the two Greek stations Penteli and Thission, but that the Perez luminous efficacy model gave better results for the stations Bratislava, Nantes and Vaulx-en-Velin. He suggests improvement by using spectral bands which are more suited to the various applications. For daylighting he believes there are enough spectral bands, but that they are not ideally defined. However, for this validation climatological values were used as input to SOLIS. A better accuracy for this version is expected when near-real-time data will be used in the near future. Table 3.10 shows a validation of global and diffuse illuminance using the Perez luminous efficacy model and the SOLIS spectral method (global illuminance only).

3.14.5 Irradiance and illuminance on a tilted plane

As part of the investigation into the applicability of the operational Heliosat-3 scheme for daylighting calculations, the accuracy of illuminance calculations for the sloped plane was investigated in [Dumortier and van Roy, 2005]. A case study for Vaulx-en-Velin showed that it was better to compute slope illuminance (especially non-south facing slopes) using sky luminance models instead of the simplified models used so far in the Satel-Light or SODA projects. In agreement with the work on luminance

Table 3.11: Summary of the results of the validations of the solar radiation parameters shown in Tables 3.6 to 3.10. The second column lists the total number of sites for which the actual parameter has been validated for the actual integration time. All values for RMSD and MBD are given as percentage of the mean observed value.

Parameter and integration time	Number of sites	Range of RMSD	Mean RMSD	Range of MBD	Mean MBD
Global irradiance					
15 minute	27	15.1 - 51.2	24.2	-15.5 - 35.6	6.4
hourly	5	13.6 - 23.1	16.1	-3.9 - 2.5	-1.1
daily sum	11	6.6 - 15.8	8.8	-9.4 - 3.8	-1.5
monthly sum	11	2.2 - 10.8	4.6	-9.4 - 3.8	-1.5
Diffuse irradiance					
15 minute	7	32.7 - 39.5	34.6	-9.3 - 0.3	-4.3
daily sum	6	14.8 - 19.5	17.1	-	-
monthly sum	6	1.9 - 10.1	5.9	-	-
Direct irradiance					
15 minute	2	35 - 37.4	36.2	-3.1 - 3	0
Global illuminance					
15 minute	5	17.2 - 32.1	22.1	-7.5 - 5.6	-0.7
Diffuse illuminance 15 minute	3	31.1 - 38.4	34.3	1.2 - 5.4	3.8

distributions, it was found that the ASRC-CIE model [Perez et al., 1992] gave the best results. This approach can probably be extended to radiance distribution and irradiances. The use of sky luminance/radiance distribution models to produce illuminances or irradiances on slopes is promising, even though it needs further validation. Having a distribution of illuminance also makes it easier to include the effect of obstructions.

3.14.6 Conclusions

The operational method was validated with pyranometer data from European meteorological stations. The average RMSE for all test-sites was 24%, 14%, 9% and 5% for 15 minute, hourly, daily and monthly data respectively. The accuracy goals set in the proposal, an RMSE of 20%, 10%, and 5%. for hourly, daily and monthly values of global horizontal irradiance have therefore been achieved.

The use of MSG-data rather than Meteosat-7 data resulted in a reduction of the RMSE of hourly data of on average 1.5%. For north-west European test sites the results of an MSG-adapted Heliosat-1 method and the operational Heliosat-3 method were comparable. For Mediterranean and Canary island test sites the Heliosat-3 method gave an RMSE reduction of two percent point, and an MBE reduction of 4 percent point.

An overview of all validations can be found in Table 3.11

A more detailed description of the validation can be found in [Dagestad et al., 2005].

3.15 Example Application: Grid Connected Photovoltaic Systems

3.15.1 The PVSAT procedure

PVSAT is a remote performance check for grid connected PV systems. No hardware installation will be necessary on site. The site specific solar irradiation data is derived from satellite images rather than from ground based measurements. On the basis of monthly irradiation time series, monthly values of PV system yield will be calculated and distributed automatically towards the system operator. He or she may then compare the estimated production to the real production meter reading.

The PVSAT procedure is based on three main components:

- A data base of PV system configuration data
- A satellite image processor
- A generic PV system model

The interaction between these components is depicted in Figure 3.11 and will be explained in the following.

A PC-based data base contains geographical, component and operator related data for each individual system. The entries in the data base cover the following details:

- Addresses of PV system site and of operator
- Geographic coordinates of the site
- Orientation and tilt angle of PV system
- Horizon obstruction at the site
- Manufacturer and type of PV modules
- Size and wiring scheme of PV generator
- Mounting technique of PV generator
- Manufacturer and type of inverter

These data are collected once for each participating system.

Global horizontal irradiation on ground is (was) estimated from the pixel values in the VIS channel of METEOSAT 5, 6, and 7. The operational PVSAT routine used a modified HELIOSAT version [Cano et al, 1986, Beyer et al., 1996], including further improvements made by the SATELLIGHT team [Hammer et al., 1998]. This version

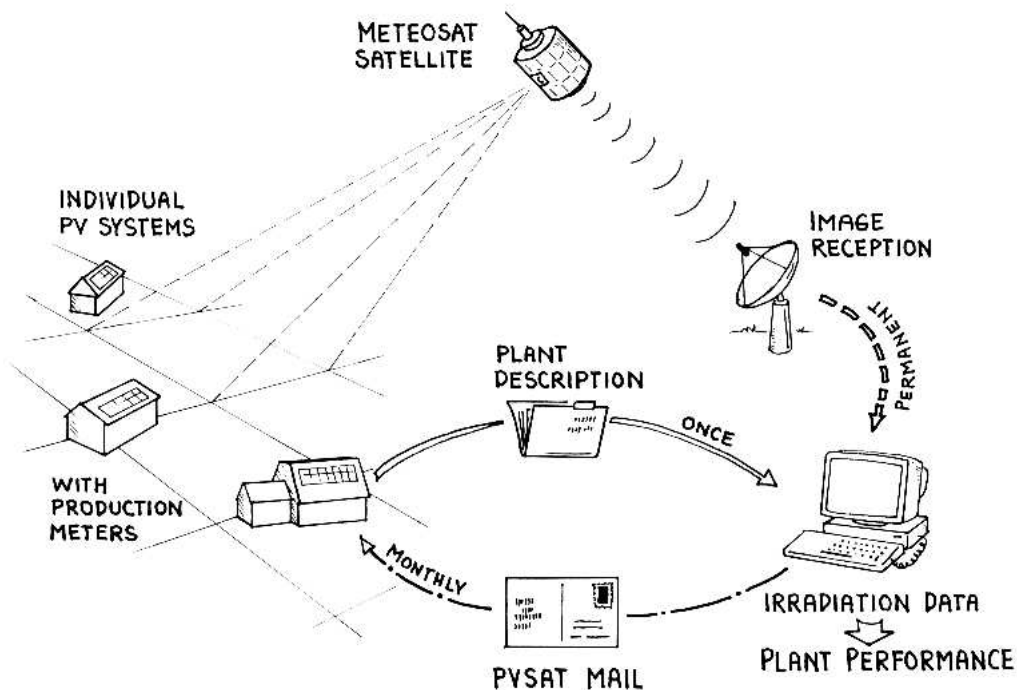


Figure 3.11: Overview on the PVSAT procedure.

was called HELIOSAT-2 sometimes. In consecutive steps, the irradiation on a horizontal plane is converted to the tilted plane irradiation, and a local horizon obstruction is taken into account.

At the end of each month, individual yield values are calculated for all PV systems. For this purpose, a generic system model is fed with the configuration data and according irradiation time series. The model has been set up using the simulation system INSEL, which has been developed by the Oldenburg University [Luther et al, 1991] and which was used for numerous system simulation and evaluation purposes [Gabler et al., 1994]. The model incorporates the following effects:

- PV IV-curve according to a 2-diode-model
- Temperature dependency of IV-curve
- Losses due to dust or soil on modules
- Ohmic losses in wiring
- Module mismatch losses
- MPP-tracking inaccuracy
- Inverter losses
- Inverter power limitation

The interface between the data base (running on MS-Windows) and the system model (running, as the satellite image processor, on Unix machines) is based on e-mail. Therefore, several distributed data bases may access the PVSAT server without interference. The results of the model calculation are transferred back to the data base, from where they are distributed (mailed, faxed or e-mailed) to the individual system operator. He or she may then compare the estimated production to the real production meter reading.

3.15.2 Algorithms and data needs

The main goal of the irradiation routine is the estimation of site specific in-plane irradiation, including effects of orientation and horizon obstructions. Additionally, information on the reliability of the irradiation values would be of great use.

Input values of global irradiation on the horizontal plane and diffuse irradiation on the horizontal plane (equivalent to the use of direct normal irradiation) are provided by the HELIOSAT-2 algorithm. Thus, the accuracy of the HELIOSAT-2 method has direct influence on the overall accuracy of PVSAT.

The calculation of irradiation on the PV module plane according to orientation, tilt angle uses the Klucher model [Klucher, 1997]. At this stage, the horizon obstruction is taken into account. The horizon line is defined as a polygon (elevation angle vs. azimuth angle) for each individual PV system. Using this polygon, the position of the sun is checked for being above or below the horizon. The diffuse irradiation is reduced proportional to the fraction of the sky vault hidden by the horizon. For this reason, the Klucher model was extended by own routines.

Result of these calculation steps is a one-month time series of 30-min (now 15-min) values of irradiation on the tilted and possibly obstructed module plane.

3.15.3 Current accuracy

Of course, there are several modelling errors contributing to the overall inaccuracy of the PVSAT routine. In previous reports on PVSAT [Reise und Wiemken, 1999], these errors were estimated as:

model step	error margin
irrad. horizontal	$\pm 9 \text{ kWh/m}^2$
irrad. tilted	$\pm 3,5 \%$
horizon influence	$\pm 5,0 \%$
PV system model	$\pm 2,5 \%$
overall error	$\pm 10 \text{ kWh/kWp}$

As the estimation of global horizontal irradiation shows higher errors during the winter months, an absolute error margin (kWh/m^2 per month) was chosen for the irradiation values instead of a relative error margin (percent of monthly sum). There-

fore, also the results of the PVSAT routine as a whole are given as XYZ kWh/kWp \pm 10 kWh/kWp.

3.15.4 Improvements in accuracy

Improvements of accuracy are surely expected with the transition from HELIOSAT-2 to HELIOSAT-3. These improvements should arise from:

- higher accuracy of global horizontal irradiation
- improved knowledge on DNI
- better representation of dynamics (15-min values)
- availability of spectral information (not used here)
- ability to detect the presence of snow (not used up to now)

The availability of spectral information is not of concern here, as there is no spectral dependency of the PV model of PVSAT.

In figures, these improvements look like this:

model step	error margin
irrad. horizontal	$\pm 7 \text{ kWh/m}^2$
irrad. tilted	$\pm 2,5 \%$
horizon influence	$\pm 4,0 \%$
PV system model	$\pm 2,5 \%$
overall error	$\pm 8 \text{ kWh/kWp}$

The overall PVSAT routine now shows a narrowed error margin: PV system yield estimations are now given as $\pm 8 \text{ kWh/kWp}$ instead of $\pm 10 \text{ kWh/kWp}$. Thus, the accuracy was increased by 20 percent via the transition from HELIOSAT-1 to HELIOSAT-3.

More improvements to be expected with the full working version of HELIOSAT-3, related to the further improved accuracy of global horizontal irradiation values and to the snow detection feature.

3.16 Example Application: Solar Thermal Power Plants

Accurate irradiance data are needed for planning e.g. photovoltaic systems or solar thermal power plants. Planners need precise information on the availability of the solar resource in order to find a good site, adjust components and to predict economic income. The efforts of the Heliosat-3 project result in very accurate irradiance data with high temporal (hourly) and spatial (1km x 1km) resolution. As an example application, the provided irradiance information is used as input for resource assessment for solar thermal power stations and for simulation of such power plants. The planning

tool STEPS (Expert System for Solar Thermal Electric Power Stations), developed at DLR, was applied to perform this example study.

3.16.1 Solar Thermal Power Plants

Solar thermal power plants use concentrating mirrors to generate high pressure steam from solar energy, in order to activate conventional steam turbines for electricity generation. As energy resource, the direct part of the solar irradiance is used (Direct Normal Irradiance DNI).

3.16.2 STEPS

STEPS (Expert System for Solar Thermal Electric Power Stations) is a planning tool to provide a systematic and efficient way of identifying and assessing potential sites for solar thermal power stations. The results of STEPS are provided in digital maps. For further data-processing and -analysing, a Geo-Information-System (GIS) is recommended. Results are e.g.:

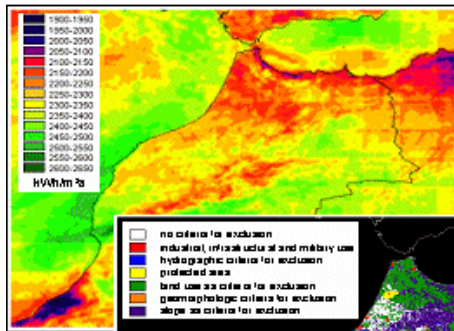
- Available solar resource
- Available land resource (shown in exclusion maps)
- Costs of infrastructure
- Costs of insurance
- Levelised Electricity Costs (LEC)

Figure 3.12 shows the main processing steps of STEPS for the example region Morocco. The working process of STEPS can be divided into several parts:

- Determination of available solar resource (Direct Normal Irradiance)
- Identifying all potential sites that are technically suitable for solar thermal power stations.
- Simulation of a solar thermal power plant for each suitable site with the determined direct solar irradiance.
- Determination of the new present value for the project
- One result is e.g. a ranking based on Levelised Electricity Cost (LEC)

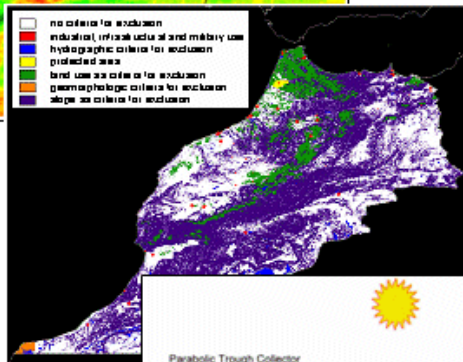
3.16.3 STEPS applied to the Canary Islands

WP 6020 aimed at the example use of the high quality irradiance data that can be provided by the new Heliosat-3 method. Here, the application was performed in the



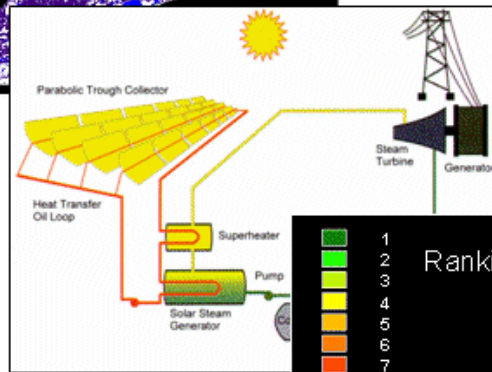
Solar Energy Resource Assessment

The beam solar radiation resource is obtained in high temporal and geographical resolution (1h, 1km) from satellite remote sensing over several years



Land Resource Assessment

Land resources are identified by a geographic information system, excluding those sites restricted by land use, land coverage, topography, hydrology, natural risks etc.



Plant Performance Modelling

Electricity yield and technical performance is modelled on hourly basis for every potential site

Economic Site Ranking

The economic ranking of all sites is defined by the resulting levelised solar electricity cost.

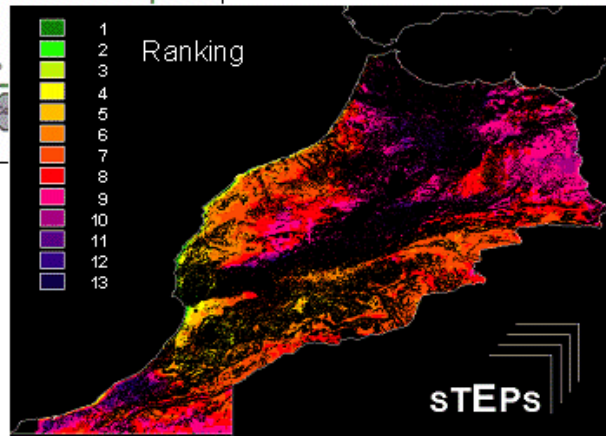


Figure 3.12: Example processing parts of STEPS for the example country analysis for Morocco. Steps from top left to bottom right: solar resource assessment (DNI), assessment of exclusion sites (white=suitable), power block simulation, ranking based on levelised electricity cost (LEC).

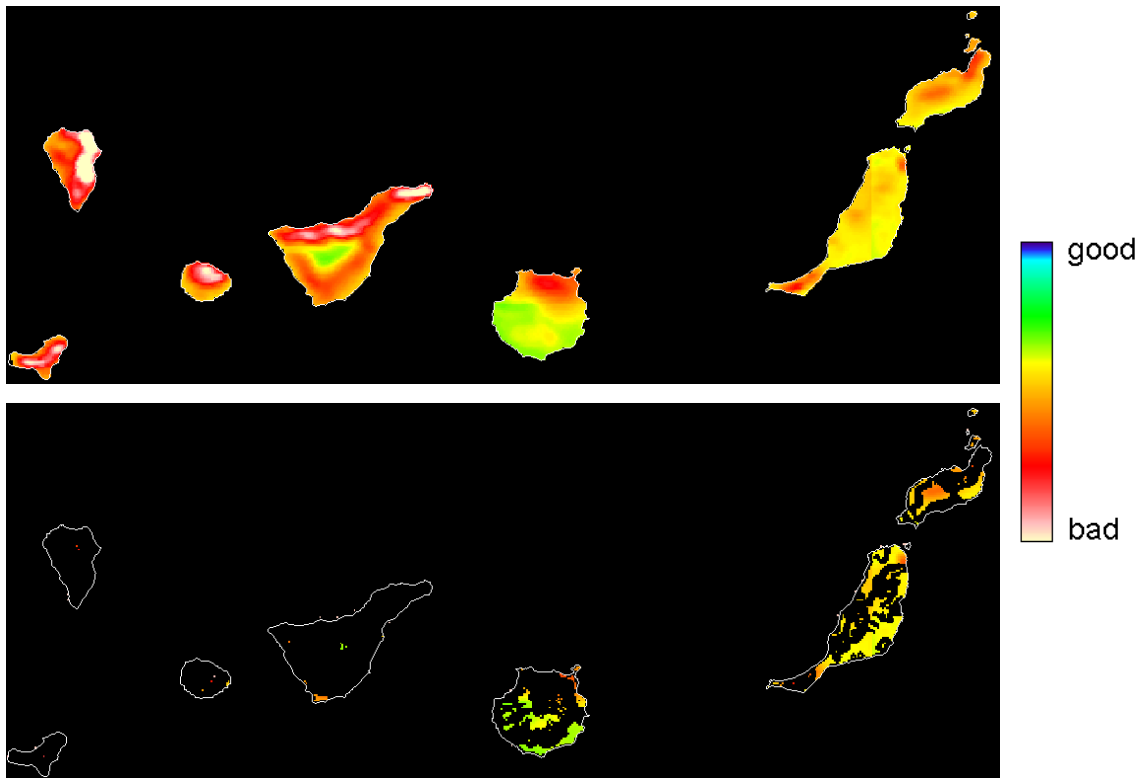


Figure 3.13: Site ranking based on Levelised Electricity Cost (LEC) for 50MW Direct Steam Generation (DSG) solar only, based on STEPS calculation, for the Canary Islands. Top figure for all sites. Bottom figure suitable sites only.

Table 3.12: Areas for Canary Islands, Gran Canaria and Fuerte Ventura. The values for non-excluded areas are based on the STEPS analysis. The solar electricity potentials are also given. They compare very favourably with the total annual electricity demand of the Canary Islands for 2005 that was predicted to be around 9 TWh/y.

Complete Area Canary Islands	7273	km ²
Non-excluded Area Canary Islands produced by STEPS	1166	km ²
Solar Electricity Potential Canary Islands	90	TWh/y
Complete Area Gran Canaria	1532	km ²
Non-excluded Area Gran Canaria produced by STEPS	302	km ²
Solar Electricity Potential Gran Canaria	25	TWh/y
Complete Area Fuerte Ventura	1731	km ²
Non-excluded Area Fuerte Ventura produced by STEPS	645	km ²
Solar Electricity Potential Fuerte Ventura	50	TWh/y

field of solar thermal power stations.

Using the STEPS-tool, the following activities were performed:

1. A first analysis for the example region Canary Islands with the internal radiation scheme of STEPS. The results show e.g. a ranking based on levelised electricity cost for a selected power plant configuration (50MW_{electric}, DSG, solar only).the software was adapted to generate maps for The internal STEPS radiation algorithm bases on Meteosat First Generation data. The method has a lower temporal and spatial resolution than the new Heliosat-3 method.
2. A second analysis. All parameter are defined as in analysis 1, but the irradiance data is now taken from the new Heliosat-3 model using data from MSG.

The results show, that the input of the new Heliosat-3 data leads to a more accurate and precise resource assessment and to a more accurate power plant simulations. The working activities within WP 6020 performed by DLR are:

1. Modifying the STEPS-tool for external irradiance data input
2. Re-organising of provided irradiance data (DNI) for efficient data processing within STEPS
3. Modifying STEPS-tool for the chosen power plant configuration
4. Modifying STEPS-tool for chosen geographic region (Canary Islands / Spain) (economic parameters)
5. Running STEPS for example region Canary Islands
6. Analysing the results

Two processing runs using the modified STEPS-tool as described above were performed for the selected region:

- One processing run using the internal irradiance scheme. For the complete year 2001, the Direct Normal Irradiance DNI was calculated within STEPS and was used as input for the STEPS power plant simulation.
- One processing run using the external irradiance data provided by Heliosat-3. For a synthetic year (based on months as described above), the Heliosat-3 DNI was used as input for the STEPS power plant simulation.

Together with the solar irradiance as input, the power block simulation, the net present value and all other available country information, the LEC can be determined. This value gives an idea about the cost for each produced kWh for the defined solar

thermal power station and for the investigated site. Figure 3.13 shows some results. The results are shown as a relative ranking with no absolute values.

The results of the study are particularly useful for energy planning by regional authorities, as they show the detailed localisation of the available solar electricity potentials of the analysed territory. They also can be used to quantify the overall electricity yield that can be achieved with different renewable energy technologies in a region. The specific renewable electricity yield of around 90 GWh/km²/y of concentrating solar power plants in the Canaries (see Table 3.12) is about 4 times higher than the equivalent area-specific electricity yield of e.g. a wind park in this region. This may be of primary concern taking into account the valuable and scarce land resources of the islands.

For every point of the map, the satellite based assessment methodology of STEPS yields an hourly time series of the solar power capacity of a solar thermal power plant. By correlating this time series with the time series of electricity demand (load curve), the capacity credit of different renewable power technologies can be evaluated. In this context, concentrating solar power plants are especially useful, as they can be build with a thermal energy for night-time operation, and additionally can be operated on the basis of conventional fuels, always guaranteeing firm capacity. Thus, they combine very well with other, fluctuating renewable energy sources like wind or photovoltaic systems, as they can be used to compensate the power fluctuations occasioned by those technologies.

Finally, the satellite resource assessment with the given quality of the HELIOSAT-3 methodology is very useful for concentrating solar power project developers, as they can make a very reliable economic analysis of the performance of the power plants prior to the investment phase. However, although the results are very accurate, it must be taken into account that the inter-annual fluctuations of solar energy can be of the order of 20-30 %. Therefore, long-term time series (> 10 years) of data are necessary to yield acceptable security for economic planning.

A more detailed description of this work can be found in [Schillings, 2005].

3.17 Example Application: Daylighting (WP 6030)

The applicability of the operational Heliosat-3 algorithm for daylighting purposes was investigated by assessment of the accuracy of the illuminance on the horizontal and tilted plane (See Sections 3.14.4 and 3.14.5). It was found that the current operational Heliosat-3 method needs further improvement to be applied for daylighting calculations.

Chapter 4

Conclusions

Objective 1: Development of a new MSG based surface solar irradiance scheme

The Heliosat-3 consortium successfully developed an operational irradiance scheme on the basis of Meteosat Second Generation data. The operational scheme consists of the new SOLIS clear sky scheme using climatological atmospheric data as input, an MSG-adapted and improved cloud index scheme and a new all weather scheme. The scheme provides spectrally resolved global horizontal irradiance, and spectrally resolved diffuse horizontal irradiance. The data has a spatial resolution of 1 km x 1km (nadir) and a temporal resolution of 15 minutes.

The clear sky scheme is based on radiative transfer modelling and provides spectrally resolved global and direct clear sky irradiance. It requires information on the aerosol, water vapour and ozone content of the atmosphere as input. In the current operational scheme climatological data are used. However, (near) real time data can be easily incorporated.

Besides technical changes to the software, adaptation of cloud index method to MSG required solving problems with the geolocation of MSG-hrv images and a new determination of empirical parameters such as the maximal cloud reflectivity and the half-width of the ground reflectivity distribution. Further improvements of the cloud index method have been developed: a correction for cloud shades, a new way to determine cloud reflectivity based on radiative transfer physics and a new statistic way to determine ground reflectivity. These improvements were not ready when the operational scheme had to be defined, but will be stepwise integrated in the operational scheme after the project.

The all-weather module includes a diffuse irradiance model that uses the newly available clear sky direct irradiance as input. Furthermore it includes a spectral look-up table to correct the spectral distribution of the clear sky irradiance for the presence of clouds.

The operational scheme differs from the scheme in the project proposal. The original 'target' scheme would have had near real time atmospheric data as input to the clear sky module and a completely new cloudy sky scheme on the basis of advanced

cloud information provided by the APOLLO scheme. Technical problems with the MSG satellite caused a large delay in the data availability. Consequently, the modules for the 'target' scheme were not ready at the start of the operationalisation and validation. However, they could be developed and validated componentwise in parallel to the validation of the operational scheme.

Objective 2: Improved accuracy

The operational method was validated with pyranometer data from European meteorological stations. The average RMSE for all test-sites was 24%, 14%, 9% and 5% for 15 minute, hourly, daily and monthly data respectively. The accuracy goals set in the proposal, an RMSE of 20%, 10%, and 5% for hourly, daily and monthly values of global horizontal irradiance have therefore been achieved.

The use of MSG-data rather than Meteosat-7 data resulted in a reduction of the RMSE of hourly data of on average 1.5%. For north-west European test sites the results of an MSG-adapted Heliosat-1 method and the operational Heliosat-3 method were comparable. For Mediterranean and Canary island test sites the Heliosat-3 method gave an RMSE reduction of two percent point, and an MBE reduction of 4 percent point.

Objective 3: New products

The SOLIS clearsky module delivers clear sky irradiance, which was not available before. A new algorithm for the all-weather direct irradiance was developed to exploit this new information. Validation showed that the new model significantly reduced the MBE of the direct and diffuse irradiance.

The new scheme provides spectrally resolved clear sky and all weather irradiance. Filter for the spectral response of the human eye (luminance), plants (PAR) and solar cells have been integrated in the software. Additional filters can be defined by the user.

A new method to derive the angular distribution of diffuse irradiance from the spatial distribution of the cloud index was developed and investigated. It was found that traditional empirical methods were more effective.

The spatial structure of the new irradiance maps has been investigated, by comparing the co-correlation of pairs of ground measurements with that of the corresponding pixels. A good agreement with the co-correlation of ground measurements was found.

Objective 4: Implementation in operational processing chains

A prototype solar energy operational chain has been running at Oldenburg University during the validation of the scheme. A stepwise-integration in the day-to day operation is ongoing.

A hybrid climatological operational chain (Helioclim-2) has been running at Ecole des Mines since February 2004. The Helioclim-2 chain has been integrated in the

SoDa service. A stepwise-integration of the complete Heliosat-3 method is ongoing.

Objective 5: Availability of cloud and atmospheric data

The APOLLO scheme, which was originally developed to use data of polar orbiting satellites, has been adapted to the MSG-SEVIRI instrument. It provides a cloud mask, cloud optical depth, cloud fraction, cloud top temperature and cloud type. The cloud fraction has been compared with NOAA-AVHRR data and an MSG-based algorithm specific for cirrus detection. Both validations showed a good agreement.

The Kleespies and McMillan method for water vapour retrieval has been adapted to the MSG-SEVIRI instrument and further improved. The method was validated on radiosonde measurements. With an RMSE of 6mm the results are in the required accuracy range.

The SYNAER method for retrieval of aerosol data retrieval has been extended further to include new and more detailed aerosol types. SYNAER using ERS-2 data has been validated on ground measured data from the AERONET network. The RMSE of the aerosol optical depth was acceptable, but the MBE of 0.1 too large. To obtain aerosol information for the observation area of MSG the SYNEAR method has been adapted to the polar orbiting satellite ENVISAT. First validation results of the SYNEAR method using ENVISAT data show a reduction of RMSE to 0.1 and a bias of zero. Further evaluation and development is currently carried out on the basis of newly available ENVISAT data.

A scheme for the retrieval of the total ozone column has been developed on the basis of the 3D global chemical-transport model DLR-ROSE 3.0 and data from ENVISAT-SCIAMACHY and ERS-2-GOME. The method was validated on ground data from the WOUDC network. The standard deviation for the GOME - WOUDC comparison is between 2.6 and 6.3 % with a mean deviation from -4.1 to 0.4 % depending on the reference station. For the SCIAMACHY - WOUDC comparison the mean deviation ranges from -8 to -0.8 % depending on the station. The standard deviation varies from 3.5 to 10.2 %.

The near real time atmospheric and cloud data are distributed via the DLR website for the research community. Furthermore, they are used in several projects the DLR is involved in.

Objective 6: User interface

The SoDa web interface has been extended to integrate the Helio-clim2 products. DLR provided a web access for the cloud and atmospheric data products to the consortium. Oldenburg University provided a web access for the irradiance products to the consortium.

Objective 7: Dissemination and exploitation

Results of the Heliosat-3 project have been integrated in the following projects and activities: the EC sponsored PVSAT-2 project, the EUMETSAT Satellite Application Facility on Climate Monitoring, the Safersun Product of Meteocontrol A.G. and the Helioclim project. The scheme is being developed further in the vIEM and ENVISOLAR projects.

The results of the project were presented in a workshop in Freiburg Germany in February 2005, and presented in technical reports, in papers in scientific Journals and at conferences.

Objective 8: Example applications

Data of the operational Heliosat-3 scheme have been applied to the PVSAT scheme for the performance control. The improved accuracy of the new scheme improved the accuracy of the calculated reference yield with 25%.

The high resolution of the new data and the improved accuracy of the direct normal irradiance product proved to be very beneficial for the investigation of the potential for solar thermal power plants with the STEPS procedure.

Daylighting applications require illuminance data as input. Validation of the illuminance product showed that a combination of the operational Heliosat-3 global irradiance in combination with an existing empirical illuminance products was more accurate than the illuminance product derived directly with the operational Heliosat-3 scheme. It is expected that a different choice of spectral bands and the use of near real time data will improve the results.

Chapter 5

Dissemination and Exploitation of the results

5.1 Dissemination

5.1.1 Website

The Heliosat-3 website (www.Heliosat3.de) is one of the tools to distribute the results of the project. All technical reports are downloadable from the site, as well as the presentation of the workshop. The internal part of the website also proved to be an effective platform for the exchange of data, software, minutes and internal reports between the partners of the Heliosat-3 project.

5.1.2 Workshop

Although the Heliosat-3 project has mainly been an scientific project, the results are of interest for the solar energy community as well as other parties with in interest in accurate irradiance data with an high spatial and temporal resolution.

5.1.3 Information package

All information about the project is downloadable from the Heliosat3 website. A CD-ROM containing the same information is available on request.

Since the Heliosat-3 project is mainly a scientific project, publications are the most important way to disseminate the results. A complete list can be found in Section 5.3.

5.2 Exploitation of results

5.2.1 EUMETSAT CM-SAF

The Satellite Application Facility on Climate Monitoring (CM-SAF) aims to generate and archive high quality data to monitor the global climate, analyse and diagnose climate parameters to understand climate change, to provide input for climate models and to validate simulation models. CM-SAF is part of the EUMETSAT funded SAF network. It is based at the Headquarters of the Deutscher Wetterdienst (DWD) in Offenbach, Germany.

An important part of climate research is understanding the radiation balance of the earth. To this aim the DWD has contracted Oldenburg University to implement the Heliosat-3 software at CM-SAF in Offenbach Germany. Part of the contractual obligation is to make a comparison between the Heliosat-3 method, the DWD satellite method and ground data. The results will be published.

5.2.2 Meteocontrol Safersun

Oldenburg University has a running contract with Meteocontrol GmbH from Augsburg, Germany to provide satellite based irradiance data. These data are used for their commercial service Safersun for the quality check of photovoltaic systems. These data are currently based on Meteosat 7 and the Heliosat-1 method. In the coming year there will be a step-wise conversion to MSG and the Heliosat-3 method.

5.2.3 Snow detection

The cloud index method (part of Heliosat-1 and the operational version of Heliosat-3) cannot distinguish between clouds and snow. Snow coverage therefore give substantial underestimation of the irradiance.

The APOLLO method which was adapted for MSG-SEVIRI as part of the Heliosat-3 method can detect snow cover. At Oldenburg University it is currently investigated how the Heliosat-1 and Heliosat-3 method can be adapted to exploit this extra investigation. Results will be implemented in normal operation, e.g the Safersun mentioned above.

5.2.4 PVSAT-2

The cloud index method is less accurate under so called "broken cloud situations". These situations were investigated, and a first approach for dealing with them was developed as part of the Heliosat-3 project. The method has been further developed and implemented in the PVSAT-2 project.

The PVSAT-2 project is an EU sponsored project for the automated quality control of grid connected PV systems.

5.2.5 vIEM

The Virtual Institute of Energy Meteorology (vIEM) addresses research at the interface between energy systems and meteorology. vIEM is run jointly by the German Aerospace Center (DLR) and the University of Oldenburg. In its initial phase, the Institute is supported by the "Impuls- und Vernetzungsfonds" of the Helmholtz Association of National Research Centers. The co-operation of Oldenburg University and DLR in this institute is a direct outcome of the HELIOSAT-3 co-operation

Within vIEM the new SOLIS clear sky irradiance algorithm is planned for integration into a solar irradiance forecasting system based on numerical weather prediction and chemical transport modelling.

Further development work how to use MSG-based cloud products for solar irradiance calculations in both cloudfree and cloudy cases will also take place within vIEM.

5.2.6 LBA

The Large Scale Biosphere-Atmosphere Experiment in Amazonia (LBA) is an international research initiative led by National Institute for Amazonian Research (INPA) from Manaus Brasil. LBA is designed to create the new knowledge needed to understand the climatological, ecological, biogeochemical, and hydrological functioning of Amazonia, the impact of land use change on these functions, and the interactions between Amazonia and the Earth system. At Oldenburg University a visiting scientist from INPA is investigating the potential of the Heliosat-3 method to generate PAR data that to be used as input to the modelling of the transport of energy and water between the atmosphere and the forest within the LBA project.

5.2.7 ENVISOLAR

ENVISOLAR is dedicated to the development of the market using information on the solar resource for planning and operations of solar energy systems. ENVISOLAR integrates the HELIOSAT-3 results in operational processing and service chains both at research and commercial partner sites. A large number of market trials performed with key customers (plant operators, plant owners, financial investors, energy suppliers) will help to further improve the operational services run by commercial partners in ENVISOLAR.

Besides from solar energy, ENVISOLAR allows also to integrate HELIOSAT-3 results on surface irradiance calculations into irradiance forecasts operated at one of the commercial ENVISOLAR partner premises. Such irradiance forecasts are delivered to energy suppliers on a regular basis and are integrated into their load forecast systems.

ENVISOLAR is funded by the ESA Earth Observation Market Development project ENVISOLAR (coordination at DLR-DFD).

5.2.8 Cloud and water vapour products at DLR

MSG-based cloud products will be used for a variety of scientific analyses e.g. climatologies and continuation of the European Cloud Climatology towards the full MSG region.

MSG-based water vapour products now available after HELIOSAT-3 will be used for atmospheric correction of remote sensing measurements from other satellites dedicated to land surface monitoring.

5.2.9 HelioClim/SoDa

HelioClim is a climatological database of irradiance data run by the Centre Energétique et Procédés de l'École des Mines de Paris. The data are accessible via the SoDa service. First steps towards integration of irradiance data based on MSG / Heliosat-3 data have been undertaken during the Heliosat-3 project. Further integration is on-going work and is carried out in co-operation with DLR.

5.3 Cumulative list of Publications

5.3.1 Peer reviewed articles

[**Dagestad and Olseth, 2006**] Dagestad, K. F., Olseth, J.: *A modified algorithm for calculating the cloud index*, Solar Energy, in print

[**Ineichen 2005**] Ineichen, P: *Broadband comparison of 8 clear sky models against 16 independent data banks* Solar Energy, in print.

[**Mueller et al., 2004**] Mueller, R.W., Dagestad, K. F., Ineichen, P., Schroedter, M., Cros, S., Dumortier, D., Kuhlemann, R., Olseth, J. A., Piernavieja, C., Reise, C., Wald, L. and Heinemann, D.: 2004, *Rethinking satellite based solar irradiance modelling - The SOLIS clear sky module*, Remote Sensing of the Environment, Vol. 91, pp. 160 - 174

[**Dagestad, 2004**] K. F. Dagestad: *Mean bias deviation of the Heliosat algorithm for varying cloud properties and sun-ground-satellite geometry*, Theoretical Applied Climatology, Vol 79, pp. 215-224.

[**Holzer-Popp et al., 2002a**] T. Holzer-Popp, M. Schroedter, G. Gesell:

Retrieving aerosol optical depth and type in the boundary layer over land and ocean from simultaneous GOME spectrometer and ATSR-2 radiometer measurements, part 1: Method description, Journal of Geophysical Research, Vol. 107, pp. D21

[**Holzer-Popp et al., 2002b**] T. Holzer-Popp, M. Schroedter, G. Gesell: *Retrieving aerosol optical depth and type in the boundary layer over land and ocean from simultaneous GOME spectrometer and ATSR-2 radiometer measurements, part 2: Case study application and validation*, Journal of Geophysical Research, Vol. 107, pp. D24

5.3.2 Theses

[**Cross, 2004**] CROS, S.: *Cratation d'une climatologie du rayonnement solaire incident en ondes courtes partir d'images satellitales*, (PhD Thesis) L'Ecole des Mines de Paris, Sophia Antipolis, France, 13-09-2004.

[**Dagestad, 2005**] Dagestad, K.F.: *Estimating global radiation at ground level from satellite images*, (PhD Thesis), University of Bergen, Norway, May 2005.

[**Girodo, 2003**] Girodo, M. *Untersuchung von 3D-Wolkeneffekten auf die satelliten-gestutzte Berechnung der solaren Einstrahlung*, (Diploma thesis), Energy and Semiconductor Laboratory, Oldenburg University, Germany, July 2003.

[**Drews, 2002**] Anja Drews: *Split-Window-Verfahren zur Ableitung von Wasserdampf-sulen aus MSG/SEVIRI und TERRA/MODIS*, (Diploma thesis), Geographisches Institut, University of Göttingen, Germany, May 2002.

[**Breitkreuz, 2005**] Hanne-Katarin Breitkreuz *Der Einfluss atmosphaerischer Partikel auf das solare Strahlungsangebot in Europa - Einsatz von Aerosolprognosen fuer energiewirtschaftliche Anwendungen*, (Diploma Thesis), Fachbereich Geowissenschaften, Universitaet Hamburg, Germany, January 2005.

5.3.3 Reports on Deliverables

[**EHF and Ecole de Mines/Armines**] Oldenburg University, Ecole de Mines/Armines, *Compilation of Data Requirements*, Oldenburg University, Germany, 30-06-2001 (includes deliverable D6).

[**EHF, 2001**] EHF, *Heliosat 3: Internet Representation of the project*, Oldenburg University, Germany, 28.09.2001 (includes deliverable D3)

[**EHF et al., 2003**] EHF, UiB, Armines, *Report of the HELIOSAT-3 software package for solar irradiance retrieval, all sky working version* Oldenburg University 28.02.2003 (includes deliverables D8.1, D8.2).

[**Schroedter- Homscheidt**] M. Schroedter- Homscheidt, L. Bugliaro, T. Erbertseder, G. Gesell, DLR T. Holzer- Popp, *Report on the Atmospheric parameter retrieval*, 31 May 2004, DLR (includes deliverables D9.1, D9.2, D9.3, D9.4).

- [**Heliosat-3 consortium, 2002**] Heliosat-3 consortium *Mid-term progress report* 29-11-2002, Oldenburg University, Germany (includes deliverables D6.1-D6.4 , D8.1 D7).
- [**Schillings, 2005**] C. Schillings, Hoyer, C., Kronshage, S., Trieb, F.: *Example Application No.2: Solar Thermal Power Plants* 2-05-2005, German Aerospace Center (DLR), Institute of Technical Thermodynamics, Stuttgart , Germany (includes deliverable D15.2).
- [**Ineichen, 2005**] Ineichen, P., *Angular distribution of the diffuse illuminance*, February 2005, University of Geneva, Switzerland (includes deliverable D11.1b).
- [**Beyer et al., 2005**] Beyer, H.G. , Betcke, J., Gallego, A.: *Treatment of topics concerning the spatial Statistics of cloud index and irradiance fields* 17 May 2005, University of Applied Sciences Magdeburg-Stendal (FH), Germany (includes deliverable D11.3).
- [**Wald, 2005**] Wald, L: *Heliosat-3 Climatology Processing Chain*, Ecole des Mines de Paris / Armines Sophia Antipolis, France (includes deliverable D13.2).
- [**Dagestad et al., 2005**] Dagestad, K-F.: *Heliosat3 Validation report* May 2005 University of Bergen, Norway (includes deliverable D16 and D15.3).
- [**Schroedter-Homscheidt et al., 2005**] M. Schroedter-Homscheidt, T. Erbertseder, G. Gesell, B. Hildenbrand, T. Holzer-Popp, W. Krebs, R., *Validation report (Atmospheric Parameters)*, German Aerospace Center (DLR), May 2005 (Appendix to Heliosat3 Validation report).
- [**Dagestad and Olseth, 2005**] Dagestad, K.F., Olseth, J.A., *An alternative algorithm for calculating the cloud index*, Geophysical institute University of Bergen, Bergen Norway, April 2005 (Appendix to Heliosat3 Validation report).
- [**Dumortier and van Roy, 2005**] Dumortier D., Roy F. van, *Models used to derive irradiances and illuminances from MSG satellite images, Comparison with measurements from 6 sites*, LASH-ENTPE, France, 2005 (Appendix to Heliosat3 Validation report).
- [**Kuhlemann and Hammer, 2005**] Kuhlemann, R, Hammer, A., *Sunsat the new program for processing high resolution data of Meteosat-8*, (Report), University of Oldenburg, Energy and Semiconductor Laboratory, June 2005.
- [**Kuhlemann and Betcke, 2005**] Kuhlemann, R, Betcke, J., *CloudS A new parameterization of radiative transfer through clouds (summary of development and first validations)*, (Report), University of Oldenburg, Energy and Semiconductor Laboratory, June 2005.

- [**Kuhlemann et al., 2005**] Kuhlemann, R, Hammer, A., Drews, A., *Geolocation of high resolution data of Meteosat-8 (VCS-XPIF format)*, (Report), University of Oldenburg, Energy and Semiconductor Laboratory, June 2005.
- [**Reise, 2005**] Reise, C: *Example Application: Grid-connected PV-systems* May 2005 Fraunhofer Institute for Solar Energy Systems, Freiburg, Germany (includes deliverable D15.1)

5.3.4 Conference papers

- [**Schroedter, 2000**] Schroedter, M.: *Water Vapour from TOVS/ATOVS - Value Added Products and Applications*, The Eleventh International ATOVS Study Conference, 20 - 26 Sept. 2000, Budapest, Hungary, Proc. pp. 357-364.
- [**Kuhlemann et al., 2002**] Kuhlemann, R., Mueller, R.W., Holzer-Popp, T., Schroedter, M., Heinemann, D.: *Is Meteosat Second Generation a candidate for aerosol detection ?* 27th General Assembly European Geophysical Society, 21-26 April 2002, Nice, France
- [**Mueller et al., 2002**] Mueller, R.W., Beyer, H.G., Dagestad, K.F., Dumortier, D., Ineichen, P., Hammer, A., Heinemann, D., Kuhlemann R., Olseth, J.A., Piernavieja, G., Reise, C., Schroedter, M., Skartveit, A., Wald, L.: *The use of Meteosat Second Generation satellite data within a new type of solar irradiance calculation scheme*, 27th General Assembly European Geophysical Society, 21-26 April 2002, Nice, France
- [**Mueller et al., 2002a**] Mueller, R.W., Heinemann, D., Kuhlemann, R., Hoyer, C., Dagestad, K.F., et al.: *A new generation of satellite based solar irradiance calculation schemes*. 22nd Symposium of the European Association of Remote Sensing Laboratories, 4-6 June 2002, Prague, Czech Republic,.
- [**Mueller et al., 2002b**] R.W. Mueller, H.G. Beyer, S. Cors, K.F. Dagestad, D. Dumortier, P. Ineichen, D. Heinemann, R. Kuhlemann, J.A. Olseth, G. Piernavieja, C. Reise, M. Schroedter, A. Skartveit, L. Wald: *The use of MSG data within a new type of solar irradiance calculation scheme*, EUMETSAT Users Conference, 2-6 September 2002 Dublin, Ireland, in: Proceedings of the 2002 EUMETSAT Meteorological Satellite Conference, pp 608.
- [**Mueller et al. 2003**] R.W. Mueller, K.F. Dagestad, R. Kuhlemann, J.A. Olseth, C. Reise, M. Schroedter, L. Wald, D. Heinemann: *Rethinking satellite based solar irradiance modelling* The 2003 EUMETSAT Meteorological Satellite Conference, 29-09 to 03-10 2003, Weimar, Germany. Proc. pp. 596-603.
- [**Cross et al., 2004**] Sylvain Cros, Marion Schroedter-Homscheidt, Thierry Ranchin, Lucien Wald: *Improvement of operational atmospheric parameters observation:*

increasing spatial resolution of aerosols optical depth maps by a data fusion process Conference of the European Meteorological Society, sept 2004.

[**Dumortier. et al., 2005**] Dumortier, D. *Estimating global irradiances and illuminances from the second generation of METEOSAT satellites - Results from the HELIOSAT-3 European project.* Confrence Lux-Europa Berlin 2005, pp. 224-226, September 19-21, 2005

[**Betcke et al., 2005**] Betcke et al. , *The results and products of the Heliosat-3 project* ECAM, Utrecht September 2005..

5.3.5 Other publications

[**Mueller et al., 2001**] *HELIOSAT-3: Solar Radiation Data from Europe's Next Satellite Generation Objectives* EU-integration meeting, (poster).

[**Baier et al. 2002**] Baier, F., Bittner, M., Schroedter, M., Erbertseder, T., Hess, M.: *Near Real Time Ozone Profiles from GOME Column Data using ROSE CTM*, 27th General Assembly European Geophysical Society, 21-26 April 2002, Nice, France (abstract and poster)

[**Holzer-Popp and Schroedter 2003a**] Holzer-Popp, T., Schroedter, M.: *Monitoring particle concentrations from space*, EGS-AGU-EUG joint assembly, 6.-11.4.2003, Nice, France (abstract).

[**Holzer-Popp and Schroedter 2003b**] Holzer-Popp, T., Schroedter, M.: *Space-based climatology of aerosol components*, EGS-AGU-EUG joint assembly, 6.-11.4.2003, Nice, France (abstract).

[**Schroedter-Homscheidt et al., 2003**] Schroedter-Homscheidt, M., Drews, A., Erbertseder, T., Gesell, G, Holzer Popp, Mannstein, H. *Towards high quality energy-specific solar radiation data from MSG - First experiences with MSG data within the Heliosat-3 project*, The 2003 EUMETSAT Meteorological Satellite Conference, 29-09 to 03-10 2003, Weimar, Germany. Proc. p. 304 (poster and abstract)

[**Dagestad, 2004**] Dagestad, K-F., *Estimating surface global radiation from Me-teosat Second Generation satellite data*, EGS conference, 5-30 April 2004, Nice, France (poster).

[**Dagestad, 2004**] Dagestad, K-F., *An algorithm for estimating global radiation from satellite measurements of TOA reflected radiance* Utrecht Climate Conference, 2001, Utrecht, the Netherlands (poster).

5.3.6 Planned publications

- [**Cros et al., 2005**] Cros S., Albuisson M., Wald L.,: *Simulating Meteosat-7 broadband radiances at high temporal resolution using two visible channels of Meteosat-8*, To be published by Solar Energy, 2005.
- [**Breitkreuz et al., 2005**] Breitkreuz, H. , Schroedter-Homscheidt, M., Holzer-Popp, T.,: *Towards the application of aerosol forecasts in the energy industries*, to be submitted to Solar Energy in June 2005
- [**Schroedter-Homscheidt and Drews, 2005**] Schroedter-Homscheidt, M., Drews, A.,: *Total water vapour column retrieval from MSG-SEVIRI split window measurements exploiting the daily cycle of land surface temperatures*, to be submitted to Remote Sensing of Environment in July 2005
- [**Girodo et al., 2005**] Girodo, M, Mueller, R, Heinemann, D: *Influence of three-dimensional cloud effects on satellite derived solar irradiance estimation - first approaches to improve the Heliosat method* accepted by Solar Energy.
- [**Kuhlemann, 2006**] R. Kuhlemann, PhD. Thesis., to be published 2006 (several chapters are to be published as Journal papers).

Bibliography

- [Beyer et al., 1996] H. G. Beyer, C. Costanzo, D. Heinemann: *Modifications of the Heliosat procedure for irradiance estimates from satellite images* Solar Energy, Vol 56 1996, pp. 207-212.
- [Beyer et al., 2005] Beyer, H.G. , Betcke, J., Gallego, A.: *Treatment of topics concerning the spatial Statistics of cloud index and irradiance fields*, (report), 17 May 2005, University of Applied Sciences Magdeburg-Stendal (FH), Germany.
- [Cano et al, 1986] D. Cano, J.M. Monget, M. Albuissou, H. Guillard, N. Regas, L.Wald: *A Method for the Determination of the Global Solar Radiation from Meteorological Satellite Data*. Solar Energy, Vol. 37, 1986, pp. 31-39.
- [Chedin et al., 1985] Chedin A., et al.: *The improved initialisation method: a high resolution physical methods for temperature retrievals from satellites of the TIROS-N series*, J. Appl. Met., Vol. 24, 1985, pp. 128-143.
- [Dagestad, 2001] Dagestad, K-F, *Ein modellstudie av sammenhengen mellom reflektert radian ved toppen av atmosfæra og globalstråling ved bakken*, Master Thesis, University of Bergen, 2001.
- [Dagestad et al., 2005] Dagestad, K-F.: *Heliosat3 Validation report* University of Bergen, May 2005.
- [Dagestad and Olseth, 2005] Dagestad, K.F., Olseth, J.A., *An alternative algorithm for calculating the cloud index*, Geophysical institute University of Bergen, Bergen Norway, April 2005 (Appendix to Heliosat3 Validation report).
- [DLR, 2000] DLR: *ENVISAT-1 SCIAMACHY Level 1c to 2 NRT and Off-line Processing Algorithm Description*, report ENV-ATB-SAO-SCI-2200-0003, Issue 2, December 2000.
- [Dubovik et al., 2002] Dubovik, O., B. Holben, T.F. Eck, A. Smirnov, Y.J. Kaufman, M.D. King, D. Tanre, I. Slutsker: *Variability of Absorption and optical Properties of Key Aerosol Types Observed in Worldwide Locations*, J. Atm. Sciences, Vol 59, 2002, pp. 590 - 608.

- [Dumortier, 1995] Dumortier D.: *Mesure, Analyse et Modélisation du gisement lumineux. Application à l'évaluation des performances de l'éclairage naturel des bâtiments*, PhD Thesis, Génie Civil et Sciences de l'Habitat, Université de Chambéry, France, December 22, 1995.
- [Dumortier and van Roy, 2005] Dumortier D., Roy F. van,: *Models used to derive irradiances and illuminances from MSG satellite images, Comparison with measurements from 6 sites*, LASH-ENTPE, France, 2005 (Appendix to Heliosat3 Validation report).
- [EHF, 2001] EHF: *Heliosat 3: Internet Representation of the project*, Oldenburg University, Germany, 28.09.2001.
- [EHF et al., 2003] EHF, UiB, Armines: *Report of the HELIOSAT-3 software package for solar irradiance retrieval, all sky working version* Oldenburg University, February 2003.
- [EHF and Ecole de Mines/Armines] Oldenburg University, Ecole de Mines/Armines: *Compilation of Data Requirements*, Oldenburg University, Germany, 30-06-2001.
- [Erbertseder, et al. 2004] Erbertseder, T., et al.: *Assimilation of ENVISAT products for continuous monitoring of atmospheric trace gases - First results from EVIVA*, submitted to ESA ERS/ENVISAT Symposium 2004
- [Erbertseder et al.,2003] Erbertseder T., F. Baier, M. Bittner, Hildenbrand, B: *Global Ozone Analyses by assimilating SCIAMACHY observations into a 3D CTM*, EGS-AGU-EGU Assembly, Nice, 2003
- [European Commission, 2000] European Commission: *Fifth Framework Programme 1998-2002, Thematic Programme Environment and Sustainable Development, Guidelines for Reporting*, 15 June 2000.
- [Fontoynt, 1998] M. Fontoynt: *Satellite: A WWW server which provides high quality daylight and solar radiation data for Western and Central Europe*, 9th Conference on Satellite Meteorology and Oceanography, Paris 1998, 434-437.
- [Gabler et al., 1994] H. Gabler, M. Raetz, E. Wiemken: *Analytical Evaluation of the Performance of Realized Photovoltaic Systems*. Proceedings of the 12th CEC PV Solar Energy Conference, Amsterdam 1994 pp.879-882
- [Gesell, 1989] Gesell G.: *An Algorithm for Snow and Ice Detection Using AVHRR Data: An Extension to the APOLLO Software Package*, International Journal of Remote Sensing, Vol. 10, 1989, pp. 897-905.

- [Girodo et al., 2005] Girodo, M, Mueller, R, Heinemann, D: *Influence of three-dimensional cloud effects on satellite derived solar irradiance estimation - first approaches to improve the Heliosat method*, Solar Energy, in print, 2005.
- [Girodo, 2003] Girodo, M. : *Untersuchung von 3D-Wolkeneffekten auf die satellitengestützte Berechnung der solaren Einstrahlung*, Diploma thesis, Energy and Semiconductor Laboratory, Oldenburg University, July 2003.
- [Govaerts and Clerici, 2004] Govaerts, Y, Clerici, M: *MSG-1/SEVIRI Solar Channel Calibration, ; Commissioning Activity Report for Eumetsat*. EUM/MSG/TEN/04/0024, Version 1.0, 21 Jan 2004.
- [Guyon et al., 2003] Guyon, P., O. Boucher, B. Graham, J. Beck, O. L. Mayol-Bracero, G. C. Roberts, W. Maenhaut, P. Artaxo, M. O. Andreae (2003): *Refractive index of aerosol particles over the Amazon tropical forest during LBA-EUSTACH 1999*, J. Aerosol Science, Vol 34, 2003, pp. 883-907.
- [Hammer et al., 1998] A. Hammer, D. Heinemann, A. Westerhellweg, P. Ineichen, J. Olseth, A. Skartveit, D. Dumortier, M. Fontoynt, L. Wald, H.G. Beyer, Ch. Reise, L. Roche, J. Page: *Derivation of Daylight and Solar Irradiance Data from Satellite Observations*. Proc. 9th Conf. on Satellite Meteorology and Oceanography, Paris 1998.
- [Hammer, 2000] A. Hammer: *Anwendungsspezifische Solarstrahlungsinformationen aus Meteosat-Daten (Application specific solar irradiance information from Meteosat data)*, Ph.D. Thesis, Carl von Ossietzky University Oldenburg, 2000.
- [Hammer et al., 2001] A. Hammer, D. Heinemann, C. Hoyer: *Effect of Meteosat VIS Sensor Properties on Cloud Reflectivity* Third SoDa meeting report, Bern, 2001.
- [Hammer et al., 2003] A. Hammer, D. Heinemann, C. Hoyer, R. Kuhlemann, E. Lorenz, R. Müller, H.G. Beyer, *solar energy assessment using remote sensing technologies*, Remote Sensing of Environment, 86, pp. 423-432, 2003.
- [Heliosat-3 consortium, 2002] Heliosat-3 consortium *Mid-term progress report 29-11-2002*, Oldenburg University, Germany.
- [Hess et al., 1998] Hess, M., Kpke, P., Schult, I., *Optical Properties of Aerosols and Clouds: The Software package OPAC*, *Bulletin of the American Meteorological Society*, Vol. 79, 1998, pp. 831-844.
- [Holben et al., 1998] Holben B.N., T.F.Eck, I.Slutsker, D.Tanre, J.P.Buis, A.Setzer, E.Vermote, J.A.Reagan, Y.Kaufman, T.Nakajima, F.Lavenu, I.Jankowiak, and A.Smirnov: *AERONET - A federated instrument network and data archive for aerosol characterization*, Rem. Sens. Environ., Vol. 66,1998, pp. 1-16..

- [Holzer-Popp et al., 2002a] T. Holzer-Popp, M. Schroedter, G. Gesell: *Retrieving aerosol optical depth and type in the boundary layer over land and ocean from simultaneous GOME spectrometer and ATSR-2 radiometer measurements, part 1: Method description*, Journal of Geophysical Research, Vol. 107, 2002, pp. D21
- [Holzer-Popp et al., 2002b] T. Holzer-Popp, M. Schroedter, G. Gesell: *Retrieving aerosol optical depth and type in the boundary layer over land and ocean from simultaneous GOME spectrometer and ATSR-2 radiometer measurements, part 2: Case study application and validation*, Journal of Geophysical Research, Vol. 107, pp. D24
- [Ineichen 2005a] Ineichen, P: *Broadband comparison of 8 clear sky models against 16 independent data banks* Solar Energy, in print.
- [Ineichen, 2005b] Ineichen, P., *Angular distribution of the diffuse illuminance*, (report), University of Geneva, Switzerland, February 2005.
- [Kato et al., 1999] Kato, S., Ackermann, T. P., Mather, J. H., Clothiaux, E. E.: *The k-distribution method and correlated-k approximation for a shortwave radiative transfer model*, J. Quant. Spectrosc. Radiat. Transfer, Vol. 62, 1999, pp. 109-121.
- [Kleespies and McMillan, 1990] Kleespies J.T. , L.M. McMillin: *Retrieval of precipitable water from observations in the Split Window over varying surface temperatures*, J. Appl. Met., Vol 29, 1990, pp. 851-862.
- [Kleespies and McMillan, 1984] Kleespies, J.T. , L.M. McMillin: *Physical retrieval of precipitable water using the Split Window technique*, Conference on Satellite Meteorology, Remote Sensing and Applications, pp. 55-57, 1984.
- [Klucher, 1997] T. M. Klucher: *Evaluation of models to predict insolation on tilted surfaces*. Solar Energy, Vol. 23(2), 1979, pp. 111-114.
- [Kriebel et al., 1989] Kriebel, K.T., R.W. Saunders and G. Gesell: *Optical Properties of Clouds Derived from Fully Cloudy AVHRR Pixels*, Beitrge zur Physik der Atmosphre, Vol. 62, No. 3, 1989, pp. 165-171.
- [Kriebel et al., 2003] Kriebel K. T., Gesell G., Kästner M., Mannstein H.: *The cloud analysis tool APOLLO: Improvements and Validation*, Int. J. Rem. Sens., Vol. 24, 2003, pp. 2389-2408.
- [Kuhlemann and Betcke, 2005] Kuhlemann, R, Betcke, J.: *CloudS A new parameterization of radiative transfer through clouds (summary of development and first validations)*, (Report), University of Oldenburg, Energy and Semiconductor Laboratory, June 2005.

- [Kuhlemann and Hammer, 2005] Kuhlemann, R, Hammer, A.: *Sunsat the new program for processing high resolution data of Meteosat-8*, (Report), University of Oldenburg, Energy and Semiconductor Laboratory, June 2005.
- [Kuhlemann et al., 2005] Kuhlemann, R, Hammer, A., Drews, A.: *Geolocation of high resolution data of Meteosat-8 (VCS-XPIF format)*, (Report), University of Oldenburg, Energy and Semiconductor Laboratory, June 2005.
- [Lorenz, 2004] Lorenz, E: *Deliverable D4.2 Improved diffuse radiation model*, report, University of Oldenburg, December 2004.
- [Luther et al, 1991] J. Luther, J. Schumacher-Gröhn: *INSEL – A Simulation System for Renewable Electrical Energy Supply Systems*, Proc. 10th CEC PV Solar Energy Conference, Lissabon, 1991, pp.457-460.
- [Mayer and Kylling, 2005] B. Mayer, A. Kylling: *Technical note: The libRadtran software package for radiative transfer calculations - description and examples of use*, Atmospheric Chemistry and Physics Vol. 5, 2005, pp. 1855-1877.
- [Mischenko et al., 2002] Mischenko, M., Penner, J., Andersen, D. (Editors), *Global Aerosol Climatology Project*, Journal of the Atmospheric Sciences, (special GACP issue) Vol 59, 2002, pp 249-778.
- [Moulin et al., 2001] Moulin, C., H. R. Gordon, V. F. Banzon, R. H. Evans (2001): *Assessment of Saharan dust absorption in the visible from SeaWiFS imagery*, J. Geophys. Res., 106, Vol. D16, 2001, pp. 18239-18249.
- [Mueller et al., 2003] Mueller, R.W., Dagestad, K. F., Ineichen, P., Schroedter, M., Cros, S., Dumortier, D., Kuhlemann, R., Olseth, J. A., Piernavieja, C., Reise, C., Wald, L. and Heinemann, D.: *Rethinking satellite based solar irradiance modelling - The SOLIS clear sky module*, Remote Sensing of the Environment, Vol. 91, 2004, pp. 160 - 174.
- [Myhre et al., 2005] Myhre, G., Stordal, F., Johnsrud, M., Diner, D. J., Geogdzhayev, I. V., Haywood, J. M., Holben, B., Holzer-Popp, T., Ignatov, A., Kahn, R., Kaufman, Y. J., Loeb, N., Martonchik, J., Mishchenko, M. I., Nalli, N. R., Remer, L. A., Schroedter-Homscheidt, M., Tanre, D., Torres, O., Wang, M., *Intercomparison of satellite retrieved aerosol optical depth over ocean during the period September 1997 to December 2000*, Atm. Chem. Phys. Disc., 2005.
- [Perez et al., 1992] Perez, R., Michalsky, J., and Seals, R.: *Modelling sky luminance angular distribution for real sky conditions. Experimental evaluation of existing algorithms*, J. Illumin. Engg. Soc., Vol. 21(2), 1992, pp. 84-92.
- [Randel et al., 1996] Randel, D. L., T. H. Vonder Haar, M. A. Ringerud, G. L. Stephens, T. J. Greenwald, and C. L. Combs: *A New Global Water Vapor Dataset*, Bull. Amer. Meteor. Soc, Vol. 77, 1996, pp. 1233-1246.

- [Reise und Wiemken, 1999] Ch. Reise, E. Wiemken: *PVSAT – Technical Report on Task 3 and Task 4*. Fraunhofer Institute for Solar Energy Systems ISE Oltmannsstrasse 5, 79100 Freiburg, Germany, November 1999.
- [Riese et al.,1999] Riese M., Tie X., Brasseur G., and Offermann D.: *Three-dimensional simulation of stratospheric trace gas distributions measured by CRISTA*, J. Geophys. Res., Vol. 104, 1999, pp. 16419-16435.
- [Rigollier et al., 2001] Rigollier, C., Lefevre, M., and Wald, L. (2001). *Heliosat version 2, Technical report*, ENSMP / T&M, report to the European Commission, 2001.
- [Rigollier et al., 2004] Rigollier C., Lefvre M., Wald L., *The method Heliosat-2 for deriving shortwave solar radiation data from satellite images*, Solar Energy, Vol 77(2), 2004, pp. 159-169.
- [Rose and Brasseur,1989] Rose K. and Brasseur G.: *A three-dimensional model of chemically active trace species in the middle atmosphere during disturbed winter conditions*, J. Geophys. Res., Vol. 94, 1989, pp. 16387-16403.
- [Saunders and Kriebel, 1988] Saunders R.W. and K.T. Kriebel: *An improved method for detecting clear sky and cloudy radiances from AVHRR data*, Int. J. Rem. Sens., Vol 9, 1988, pp. 123-150.
- [Schillings, 2005] C. Schillings, Hoyer, C., Kronshage, S., Trieb, F.: *Example Application No.2: Solar Thermal Power Plants 2-05-2005*, German Aerospace Center (DLR), Institute of Technical Thermodynamics, Stuttgart , Germany.
- [Schnaiter et al., 2003] Schnaiter, M., H.Horvath, O. Mhler, K.-H. Naumann, H. Saathoff, O.W. Schck: *UV-VIS-NIR spectral optical properties of soot and soot-containing aerosols*, J. Aerosol Science, Vol. 34, pp. 1421-1444, 2003.
- [Schroedter- Homscheidt, 2004] M. Schroedter- Homscheidt, L. Bugliaro, T. Erbertseder, G. Gesell, DLR T. Holzer- Popp, *Report on the Atmospheric parameter retrieval*, 31 May 2004, DLR, Germany.
- [Schroedter-Homscheidt et al., 2005] M. Schroedter-Homscheidt, T. Erbertseder, G. Gesell, B. Hildenbrand, T. Holzer-Popp, W. Krebs, R., *Validation report (Atmospheric Parameters)*, German Aerospace Center (DLR), May 2005 (Appendix to Heliosat3 Validation report).
- [Shettle and Fenn, 1976] Shettle, P., Fenn, R. W.: *Models of the atmospheric aerosols and their optical*, AGARD Conference Proceedings on optical propagation in the atmosphere, Vol.183, 1976.
- [Sinyuk, 2003] Sinyuk, A., O. Torres, O. Dubovik: *Combined use of satellite and surface observations to infer the imaginary part of refractive index of Saharan dust*, GRL, Vol 30, No 2, 1081, doi 10.1029/2002GL016189, 2003.

- [Simpson et al., 2001] Simpson, J. J., J. S. Berg, C. J. Koblinsky, G. L. Hufford, and B. Beckley: *The NVAP global water vapor dataset: Independent cross-comparison and multiyear variability*, Remote Sensing of Environment, Vol. 76, 2001, 112-129.
- [Skartveit et al., 1998] Skartveit, A. and Olseth, J.A., Tuft, M.E.: *An hourly diffuse fraction model with correction for variability and surface albedo*, Solar Energy, Vol. 63, pp. 63, 1998
- [Wald, 2005] Wald, L: *Heliosat-3 Climatology Processing Chain*, Ecole des Mines de Paris / Armines Sophia Antipolis, France (includes deliverable D13.2).
- [woudc,2005] <http://www.woudc.org>.

Appendix A

Participant Information

Partners in the Heliosat-3 project

University of Oldenburg
Faculty of Physics
Energy and Semiconductor Research Laboratory
(EHF)

D-26111 Oldenburg (Oldb)
Germany
fax: ++49 441 798 3326
web: <http://www.energiemeteorologie.de>

- Dr. Detlev Heinemann
detlev.heinemann@uni-oldenburg.de
tel: ++49 441 798 3543
- Jethro Betcke
jethro.betcke@uni-oldenburg.de
tel: ++49 441 798 3927
- Rolf Kuhlemann
rolf.kuhlemann@uni-oldenburg.de
tel: ++49 441 798 3929
- Dr. Richard Mueller
(Currently employed at German Weather Service, DWD)
richard.mueller@dwd.de
tel: ++ 49 698 062 4922

**Ecole des Mines de Paris / Armines
Groupe Teledetection et Modelisation**

BP 207

F-06904 Sophia Antipolis cedex

France

fax: ++ 33 4 93957535

web: <http://www-cenerg.cma.fr/eng/tele> or [fr/tele](http://www-cenerg.cma.fr/fr/tele)

- Prof. Lucien WALD
lucien.wald@ensmp.fr
tel: ++33 4 93957449
- Dr. Sylvain Cros
sylvain.cros@ensmp.fr

**Deutsches Zentrum für Luft- und Raumfahrt
Deutsches Fernerkundungsdatenzentrum
(DLR-DFD)**

Postfach 1116

D-82234 Wessling

Germany

fax: ++ 49 8153 28 1363

web: <http://www.dfd.dlr.de> and <http://wdc.dlr.de/>

- Marion Schroedter-Homscheidt
marion.schroedter-homscheidt@dlr.de
tel: +49-8153-28-2896
- Dr. Thomas Holzer-Popp
Thomas.holzer-popp@dlr.de
- Thilo Erbertseder
thilo.erbertseder@dlr.de
- Beate Hildenbrand
beate.hildenbrand@dlr.de
- Miriam Kosmale

**University of Bergen
Geophysical institute
(UiB-GI)**

Allegt. 70
N-5007 Bergen
Norway fax: +47 55589883 web: <http://www.gfi.uib.no>

- Jan Asle Olseth
jan.asle.olseth@gfi.uib.no
tel: +47 55582892
- Dr. Knut-Frode Dagestad
(Currently employed at Nansen Environmental and Remote Sensing Center)
knutfd@nersc.no
tel: ++ 47 5520 5868

**University of Geneva
Group of Applied Physics
(UNIGE)**

Battelle Btiment A
7 route de Drize
1227 Carouge - Geneve
Switzerland
fax: ++ 41 22 379 06 39 web: <http://www.unige.ch/cuepe/>

- Dr. Pierre Ineichen
pierre.ineichen@cuepe.unige.ch
tel: ++ 41 22 379 06 40

**Fraunhofer Institute for Solar Energy Systems
(FhG-ISE)**

Heidenhofstrasse 2
D-79110 Freiburg
Germany
fax: ++ 49 761 4588 9282
web: <http://www.ise.fhg.de>

- Dr. Christian Reise
christian.reise@ise.fraunhofer.de
tel: ++ 49 761 4588 5282

**Ecole Nationale des Travaux Publics de l'Etat
Centre Nationale de la Recherche Scientifique
Département Génie Civil et Bâtiment
(ENTPE-CNRS-DGCB)**

rue Maurice Audin
F-69518 Vaulx-en-Velin, Cedex
France
fax: ++ 33 4 72047041
web: <http://www.entpe.fr/Prive/index-recherche.htm>

- Dr. Dominique Dumortier
dominique.dumortier@entpe.fr
tel: +33 4 72047087

**Canary Islands Technological Institute
Energy, Water and Bioengineering Division
Renewable Energies Department
(CIEA-ITC)**

Playa de Pozo Izquierdo s/n
Pozo Izquierdo
E-35119 - Santa Luca
Las Palmas
Gran Canaria
España
fax: ++ 34 928 727517
web: <http://www.itccanarias.org>

- Antonio Ortegón Gallego
aortegon@itccanarias.org
tel: +34 928 7275 18/03

subcontracters

**Hochschule Magdeburg-Stendal (FH)
Fachbereich Elektrotechnik**

Breitscheidstrasse 2
D-39114 Magdeburg
Germany
fax: web: <http://www.elektrotechnik.hs-magdeburg.de/>

- Prof. Dr. Hans Georg Beyer
hans-georg.beyer@et.hs-magdeburg.de
tel: +49 391 8864499

**Deutsches Zentrum für Luft- und Raumfahrt
Institut für Technische Thermodynamik
(DLR-TT)**

Pfaffenwaldring 38-40
D-70569 Stuttgart
Germany
fax: ++ 49 711 6862 783
web: <http://www.dlr.de/tt/>

- Franz Trieb
franz.trieb@dlr.de
tel: +49 711 6862 423
- Carsten Hoyer
carsten.hoyer@dlr.de tel: +40 711 6862 784
- Christoph Schillings
christoph.schillings@dlr.de
tel: +49 711 6862 784

**Deutsches Zentrum für Luft- und Raumfahrt
Institut für Physik der Atmosphäre
(DLR-PA)**

Postfach 1116
D-82230 Wessling
Germany
fax: ++ 49 8153 28 1363
web: <http://www.dlr.de/ipa/>

- Hermann Mannstein
Hermann.Mannstein@dlr.de
- Luca Bugliaro
Luca.Bugliaro@dlr.de

Appendix B

Glossary

AATSR	Advanced Along Track Scanning Radiometer
AERONET	NASA's Aerosol Robotic Network
AOD	Aerosol Optical Depth
AOT	Aerosol Optical Thickness (same as AOD)
APOLLO/AVH	AVHRR Processing scheme Over cLOUDs Land and Ocean for AVHRR
APOLLO/SEV	AVHRR Processing scheme Over cLOUDs Land and Ocean for SEVIRI
ATSR	Along Track Scanning Radiometer
AVHRR	Advanced Very High Resolution Radiometer
BADC	British Atmospheric Data Centre
BLAOT	Boundary layer aerosol optical thickness
BMU	Bundes Ministerium für Umwelt, Naturschutz und Reaktorsicherheit German Ministry of the Environment, Nature Protection and Reactor Security
DOAS	Differential Optical Absorption Spectroscopy
DNI	Direct Normal Irradiance
ECMWF	European Center for Middle-Range Weather Forecasting
ENVISOLAR	Environmental Information Services for Solar Plant Management (www.envisolar.com), ESA supported project
ERS	European Radar Satellite
ESA	European Space Agency
EUMETSAT	European Organisation for the Exploitation of Meteorological Satellites
GDP	GOME data processor
GIS	Geographical Information System
GOME	Global Ozone Monitor Experiment
HRIT	High Rate Information Transmission, data format in which MSG data is transmitted
HRV	High Resolution Visible, broadband channel of MSG SEVIRI
LBA	Large Scale Biosphere-Atmosphere Experiment in Amazonia (http://lba.inpa.gov.br)
Level 1.0 data	Image data as acquired by the MSG satellite

Level 1.5 data	before any ground processing has taken place. data derived from the Level 1.0 data that is acquired by the MSG satellite and received by EUMETSAT's ground segment. EUMETSAT corrects in real-time each received Level 1.0 image for all radiometric and geometric effects and geolocates it using a standardised projection.
Level 2 data	Geophysical and atmospheric data produced using the Level 1.x data radiances as input
Level 3 data	Gridded data that has been statistically collected into daily, weekly, monthly, or annual grid cells
MeCiDA	MSG Cirrus Detection Algorithm
MLB	Modified Lambert Beer
MODIS	Moderate Resolution Imaging Spectroradiometer
MSG	Meteosat Second Generation
Nadir	Directly below satellite
NASA	National Aeronautics and Space Administration
NOAA	National Oceanic and Atmospheric Administration
NRT	Near Real Time
OPAC	Optical Properties of Aerosols and Clouds (database)
PAR	Photosynthetically Active Radiation, range of the solar spectrum that is used by the photosynthesis in plants.
RTM	Radiative transfer modelling
RMSE	Root Mean Square Error, measure for the overall accuracy
RMSD	Root Mean Square Deviation, measure for the overall accuracy
SCIAMACHY	Scanning Imaging Absorption Spectrometer for Atmospheric Cartography Instrument on board of Envisat
SEVIRI	Spinning Enhanced Visible and Infra Red Imager Instrument on board of MSG
SOLIS	SOLAR Irradiance Scheme
STEPS	Expert System for Solar Thermal Electric Power Systems GIS based tool to analyse the technical and economical potential of these systems
SYNAER	SYNERgetic AErosol Retrieval
TIGR	Thermodynamic Initial Guess Retrieval
OMS	Total Ozone Monitoring Spectrometer
TWC	total water vapour column
UTC	Universal Time Coordinated
VCS	VCS Aktien Gesellschaft, supplier of Meteosat reception hardware and software (www.vcs.de)
vIEM	Virtual Institute of Energy Meteorology (www.viem.de)
XPIF	eXtended Processed Image File architecture, data format to which the VCS reception software saves the satellite data

Appendix C

Workshop Program

Heliosat-3: Increasing Solar Energy Value with Satellites

Outcome of the European Heliosat-3 Project

Fraunhofer Institute for Solar Energy Systems

Freiburg, Germany 23 February 2005

09:30 Reception

General session

09:50 Welcome and Introduction

10:00 Opening

(Prof . Joachim Luther, Fraunhofer Institute for Solar Energy Systems)

10:15 Satellite Data and it's Use for Solar Energy Applications

(Dr. Antoine Zelenka, MeteoSwiss)

11:00 Coffee break

11:30 Introduction to the Heliosat-3 project: Science, results and products.

(Jethro Betcke, Oldenburg University)

Implementation session

12:00 Implementation and commercialisation of the Heliosat-3 results in the ENVISO-LAR project.

(Marion Schroedter-Homscheidt, German Aerospace Centre DLR)

12:30 Lunch

14:00 Climatological data derived from satellites

(Prof. Lucien Wald, Ecole des Mines de Paris / Armines)

Applications Session

- 14:30 Solar irradiance data in architecture: Optimisation of daylight use.
(Dr. Dominique Dumortier, Ecole Nationale des Travaux Publics de l'Etat)
- 15:00 Solar irradiance data and quality control of grid connected PV
(Gerd Heilscher, Meteocontrol GmbH)
- 15:40 Coffee break
- 16:00 Solar thermal power plants.
(Carsten Hoyer, German Aerospace Centre DLR)
- 16:30 Application in climate research
(Dr. Richard Mueller, German Weather Service DWD)
- 17:00 Outlook and opportunities
(Dr Detlev Heinemann, Oldenburg University)
- 17:15 Open Discussion: Needs of the Solar Energy Industry
- 18:00 End

The presentations can be downloaded from <http://www.heliosat3.de>